

Choosing the consolidant for carbonate substrates: Technical performance and environmental sustainability of selected inorganic and organic products

Giulia Masi, Alessandro Dal Pozzo, Greta Ugolotti, Alessandro Tugnoli, Enrico Sassoni*

Department of Civil, Chemical, Environmental and Materials Engineering (DICAM), University of Bologna, Via Terracini 28, 40131 Bologna, Italy

ARTICLE INFO

Keywords:

Hydroxyapatite
Ammonium phosphate
Calcium phosphates
Nanolimes
Ethyl silicate
Acrylic resin
Paraloid B72
Consolidation
Life cycle assessment
LCA

ABSTRACT

This study aims at providing a dataset for selecting the most suitable consolidant for marble, limestone and lime mortar. Diammonium hydrogen phosphate (DAP), nanolimes (NL), ethyl silicate (ES) and acrylic resin (B72) were compared. Application was performed by brushing in different amounts to investigate the influence of the product consumption. Effectiveness, compatibility, durability and sustainability were evaluated. DAP showed several advantages over the alternative consolidants, in terms of both technical performance and sustainability. ES exhibited high efficacy but also risks of poor compatibility and durability, together with a high global warming potential. NL and B72 provided the least promising results.

1. Introduction

Natural stones and mortars used in historical architecture and sculpture suffer from deterioration when exposed outdoors, the type and the intensity of the decay processes depending on the properties of the substrate and the environmental conditions. Marble, owing to its very low porosity, is subject to thermal weathering induced by repeated heating-cooling cycles [1]. Porous substrates, such as porous limestone and slaked lime mortars, generally suffer from stress induced in the pores by freezing-thawing and salt crystallization cycles [2].

To arrest deterioration and possibly prevent further decay, consolidants are often applied. Consolidants are liquid products that penetrate into the deteriorated substrate and, after hardening, increase its cohesion, thus improving its mechanical properties and its resistance to deterioration processes. In principle, the ideal consolidant should be *effective* (i.e. able to provide a significant strengthening action), *compatible* (i.e. not causing undesired changes in color, pore size distribution and physical properties), *durable* (i.e. maintaining its strengthening action over time, without releasing undesired by-products), *removable* or at least *reatreatable* (i.e. it should not prevent the possibility of applying a different treatment in the future) [3,4]. Moreover, an additional requirement that is acquiring increasing

importance is the *sustainability* of the consolidating treatment (i.e. it should have a reduced impact on the environment) [5].

To simultaneously fulfill all these requirements is extremely challenging, hence the selection of the best consolidant to be applied on a certain monument is far from being straightforward [6]. In some cases, the compatibility requirement is considered as the most important one, so new consolidants have been regarded as promising based on the fact that the final product formed after hardening is compatible with the substrate and reduces its porosity, even though its actual strengthening efficacy has not been specifically quantified [7]. In other cases, a high consolidating ability is considered as extremely important, so certain consolidants are still used in the conservation practice because of their high effectiveness, despite known compatibility and durability issues, which have led to the urgent need of removing unsuitable consolidants applied in the past decades [8].

Once the most promising consolidant for a certain substrate has been selected, a further delicate aspect is the amount of product to apply, as this may significantly influence the treatment outcome [9]. The technical data sheets of commercial products usually recommend application until apparent refusal, i.e. until the substrate no longer absorbs the liquid consolidant. However, in the case of highly porous substrates, treatment until apparent refusal may require a very high number of

* Corresponding author.

E-mail address: enrico.sassoni2@unibo.it (E. Sassoni).

applications (e.g. 50 brush strokes), which may not always be feasible for technical and economic reasons and actually may negatively affect the compatibility of the treatment (i.e. resulting in visible color change). Therefore, a lower number of applications is often applied [9], which influences the pore filling, the strengthening ability, the color change and also the environmental sustainability of the intervention (e.g. by halving the number of applications, the risk of color change and the environmental impact are reduced, but in turn the strengthening effectiveness may be significantly reduced as well).

To provide a dataset that can guide the selection of the most suitable consolidant to be applied onto a certain substrate, in the present study we systematically evaluated the effectiveness, compatibility, durability and sustainability of four consolidants (three inorganic products and an organic one), when applied onto marble, limestone and slaked lime mortar, artificially decayed to resemble the condition of substrates needing consolidation. Moreover, to investigate the effects of reducing the product consumption with respect to the recommended application until apparent refusal, all the consolidants were applied in three different quantities, defined based on the porosity and the absorption of each type of substrate. The four consolidants considered in the study were:

- Diammonium hydrogen phosphate (DAP), which is receiving increasing attention because of its several advantages compared to traditional products [10]. The principle of this consolidant is to treat the substrate with an aqueous solution of DAP, which provides phosphate ions to react with calcium ions coming from the substrate, to form new calcium phosphates with binding ability [11].
- Nanolimes (NL), which have been originally proposed for consolidation of wall paintings but are now used for consolidation of all types of carbonate substrates [12]. The principle is to treat the substrate with an alcoholic dispersion of $\text{Ca}(\text{OH})_2$ particles, reduced to the nanoscale to facilitate penetration, which transform into CaCO_3 upon reaction with atmospheric CO_2 [12].
- Ethyl silicate (ES), which is the most widely used product for consolidation of silicate substrates but is frequently applied also on carbonate ones [13]. The principle of this consolidant is to treat the substrate with ethyl silicate oligomers (often dissolved in an organic solvent) that undergo hydrolysis-condensation reactions, thus forming a silica gel that can chemically bond to silicate substrates [13].

- Acrylic resin (B72), which has been used as an adhesive and a consolidant for various types of substrate for several decades [14] and is still frequently used nowadays. The principle of this consolidant is to treat the substrate with a solution of acrylic resin in an organic solvent (typically acetone), followed by solvent evaporation and solidification of the resin.

2. Materials and methods

The experimental approach of this study is summarized in the schematic reported in Fig. 1.

2.1. Specimens

2.1.1. Marble and limestone

Carrara marble (a calcitic marble with some quartz and dolomite impurities (Fig. S1) and with $\sim 3\%$ open porosity, assessed by mercury intrusion porosimetry (MIP) as described in Section 2.3.2.2) and Lecce stone (an organogenic limestone, also containing quartz and fluorapatite fractions (Fig. S1), with $\sim 26\%$ open porosity, as assessed by MIP) were selected for the experimental tests, as they have been widely used in historic architecture and sculpture, they suffer from severe deterioration when exposed outdoors and hence are often in need of consolidation. Because of their different microstructure, these lithotypes are susceptible to different decay processes (mostly thermal weathering for Carrara marble [1] and salt weathering for Lecce stone [15]), hence they were selected as representative of stones with low and high porosity, respectively. The surface roughness of the two substrates was characterized by using the parameter R_c (in μm), which represents the mean value of heights from peak to valley of the roughness profile (10 mm length, 5 replicates per condition), assessed by using an optical profilometer (Leica Dual Core Microscope DCM 3D). The marble samples exhibited a significantly smoother surface ($R_c = 8.7 \pm 0.9 \mu\text{m}$) than limestone ones ($R_c = 30.9 \pm 4.0 \mu\text{m}$).

Cylindrical specimens (50 mm diameter, 20 mm height) were core-drilled from a single slab of each lithotype. To simulate the condition of naturally weathered stones, before applying the consolidants all the specimens were artificially weathered by heating in an oven at 250°C for 3 h, according to a previously developed method [11]. During heating, the anisotropic deformation of calcite crystals causes micro-crack formation at grain boundaries, with a consequent decrease in

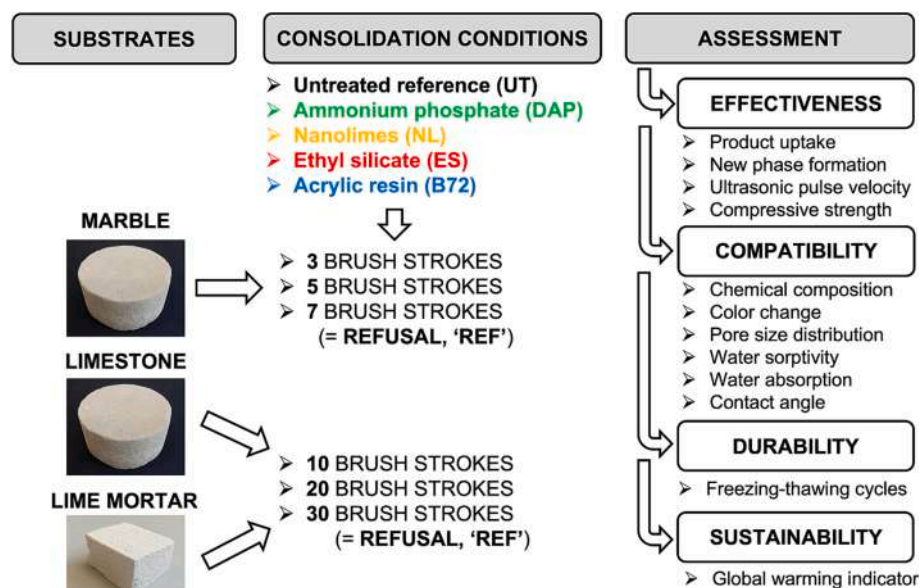


Fig. 1. Scheme illustrating the rationale of the study.

cohesion and mechanical properties [11]. Artificial weathering by heating was preferred over alternative methods (e.g. salt weathering), because in this way the decayed specimens exhibited microcracks to be sealed by the consolidants, without being contaminated by foreign ions that might alter the expected hardening reactions of the consolidants.

2.1.2. Mortar

Mortar specimens were prepared with the twofold goal of resembling the features of historic mortars and having sufficient mechanical properties to be handled for laboratory operations. Among the binder-to-aggregate ratios reported in the literature for historic mortars, generally ranging from 1:3 to 1:2, the latter ratio was selected. Such a ratio has been reported, for instance, in historic mortars in Crete [16], in Hagia Sophia in Istanbul [17] and in the most superficial layers of mural paintings (the so-called “*Intonaco*” and “*Intonachino*”), when these layers had limited thickness [18]. Although the 1:2 binder-to-aggregate ratio generally corresponds to good mechanical properties of the mortar, while consolidants should be preferably tested on substrates with poor mechanical properties (hence needing consolidation), still mortars prepared with a 1:2 ratio were regarded as a fair compromise between the competing needs of having samples representative of historic mortars needing consolidation and having samples suitable for operations in the laboratory activity. A water-to-binder ratio of 1:1 v/v (0.45 w/w) was adopted.

The fresh mortar was prepared in a Hobart mixer, using slaked lime (CL 70-S by Colacem, Italy) and calcareous sand (maximum particle size of 4 mm). The fresh mortar was poured in purposely-built molds, manually compacted and leveled. The specimens ($30 \times 20 \times 160 \text{ mm}^3$) were then immediately removed from the molds and cured for 4 months in a climatic chamber ($\text{RH} = 90 \pm 2\%$ and $T = 21 \pm 2^\circ\text{C}$), before being further cured for additional 3 months in laboratory conditions ($\text{RH} = 50 \pm 5\%$ and $T = 21 \pm 2^\circ\text{C}$). The specimens were then hand sawn to obtain $30 \times 30 \times 20 \text{ mm}^3$ samples, which exhibited a final open porosity $\sim 21\%$, as assessed by MIP. The resulting mortar samples exhibited higher surface roughness ($R_c = 42.1 \pm 3.9 \mu\text{m}$) than the two stone types.

2.2. Consolidating treatments

Four consolidants (three inorganic and one organic products) were applied onto the three types of substrate, considering triplicate specimens for each test:

- DAP. Commercial diammonium hydrogen phosphate (DAP, $(\text{NH})_4\text{HPO}_4$), supplied by C.T.S. s.r.l., Italy) was used as received to prepare a 3 M DAP solution in deionized water. The solution was brushed onto the specimens for the intended number of applications (detailed below), then the samples were wrapped in a plastic film for 24 h to allow for reaction without evaporation of the DAP solution. The samples were then unwrapped, rinsed with water, and dried at room temperature. Once dried, the treated surface was covered with a sheet of Japanese paper and then a poultice of cellulose pulp and limewater (1:4 w/w) was applied. The specimens were again wrapped in a plastic film for 24 h, to allow for limewater penetration into the pores and reaction between unreacted DAP and Ca^{2+} ions present in limewater [19]. Then, the specimens were unwrapped, and the limewater poultice was left to dry on the specimens, so that still unreacted fractions could be transported into the poultice during drying [19]. The samples were finally rinsed with water and dried at room temperature.
- NL. The commercial product Nanorestore Plus® Ethanol 5 (supplied by C.T.S. s.r.l., Italy), consisting in a dispersion of $\text{Ca}(\text{OH})_2$ nanoparticles in ethanol with 5 g/L concentration, was used as received. The nanoparticle dispersion was brushed onto the specimens for the intended number of applications, after covering the surface to be treated with a sheet of Japanese paper to prevent whitening, as recommended in the technical data sheet. Again, following the

recommendation by the producer, at the end of the application a poultice of cellulose and deionized water (1:4 w/w) was applied onto the Japanese paper, to favor carbonation. After the poultice dried, the specimens were left to cure in laboratory conditions for 4 weeks, as recommended in the technical data sheet.

- ES. The commercial product ESTEL 1000 (supplied by C.T.S. s.r.l., Italy), containing 75 wt% ethyl silicate with also 1 % dibutyltindilaurate as catalyst and 25 wt% white spirit, was applied as received. The product was brushed onto the specimens for the intended number of applications, then the specimens were left to cure in laboratory conditions for at least 4 weeks, as recommended in the technical data sheet.
- B72. The commercial product PARALOID® B72 (supplied by C.T.S. s.r.l., Italy), consisting of 100 % ethyl-methacrylate copolymer, was used as received to prepare a 5 wt% solution in acetone. The solution was brushed onto the specimens for the intended number of applications and then excessive product accumulated on the surface was removed by using acetone applied by brush.

The consolidants were brushed onto one circular face in the case of marble and limestone and one square face ($30 \times 30 \text{ mm}^2$) in the case of lime mortars using a conventional 40 mm-brush, waiting for the product to be absorbed between subsequent strokes. For each type of substrate, three conditions were considered, corresponding to an increasing number of brush strokes, namely 3, 5 or 7 for marble and 10, 20 or 30 for limestone and mortar (Fig. 1). The highest number of brush strokes corresponded to apparent refusal, intended as the condition when the operator visually observed the specimen surface remaining wet for more than 1 min after a single brush stroke [20]. When the consolidants were applied until apparent refusal, the possible excess product on the sample surface was removed by rinsing with the respective pure solvent.

While for NL and ES information on the consolidant viscosity is provided by the suppliers, in the case of DAP and B72 solutions the viscosity was determined experimentally, by measuring the volumetric flux of the consolidant through a capillary tube with known diameter and known length, for a given liquid head, at room temperature ($T = 25^\circ\text{C}$). The resulting viscosity values (in mPa·s) decrease in the order $\text{ES} = 10 > \text{DAP} = 2.9 > \text{NL} = 2.7 > \text{B72} = 0.8$ (for reference's sake, water viscosity is 1 mPa·s).

2.3. Specimen characterization

2.3.1. Effectiveness

2.3.1.1. *Product consumption.* The product consumption (in L/m^2) was assessed by weighing beakers with the various consolidants, before and after application onto all the specimens by brushing. From the weight measurement, the volume of liquid consolidant consumed for each product was calculated based on the respective densities.

2.3.1.2. *Product uptake.* The product uptake by the specimens (in L/m^2) was assessed by weighing the specimens before and after brushing the consolidants.

2.3.1.3. *Dynamic elastic modulus (E_d).* Taking advantage of its non-destructive nature, E_d was determined on each specimen, before and after treatment. The ultrasonic pulse velocity, UPV, was measured by transmission method across the specimens, by using a PUNDIT instrument with 55 kHz transducers. The transducers were placed in the center of the two circular faces, in the case of the stone samples, and in the center of the square faces, in the case of the mortar samples. E_d was then calculated using the formula $E_d = \rho \times \text{UPV}^2$, where ρ is the geometric density.

2.3.1.4. *Compressive strength by double punch test ($\sigma_{c,DPT}$).* The

compressive strength by DPT was determined by loading the specimens with two circular steel plates (20 mm diameter), placed in the center of the circular faces (stones) and square faces (mortars). The size of the plates was selected based on a previous study [21], which showed that a more reliable evaluation of the compressive strength is obtained when the diameter of the plates (20 mm) is equal to the thickness of the specimens (20 mm for both the stone and the mortar specimens). The compressive load was progressively increased until failure by using a Galdabini loading machine and the $\sigma_{c,DPT}$ was calculated as the ratio of the failure load to the circular area of the steel plates.

2.3.1.5. Composition of the new phases. The composition of the new phase formed by the various consolidants was investigated by Fourier Transform Infrared Spectrometry (FT-IR) and by X-Ray Diffraction (XRD). FT-IR was performed on powder obtained by scratching with a spatula from the surface of specimens that had been subjected to the water absorption test and then mechanical testing, by using a Perkin Elmer Spectrum Two instrument (ATR mode, 4000–400 cm^{-1} range, spectral resolution 4 cm^{-1} , 16 scans, data interval 1 cm^{-1}). The acquired FT-IR spectra were normalized with respect to the calcite band at 872 cm^{-1} . XRD was performed on untreated and consolidated surfaces of sample fragments, by using a Malvern PANalytical Empyrean X-ray diffractometer equipped with a Cu tube (K_{α} radiation $\lambda = 1.5405 \text{ \AA}$). The experimental parameters were as follows: generator voltage = 40 kV, tube current = 30 mA, $2\theta = 4\text{--}45^\circ$, step size = 0.013° and time per step = 48 s.

2.3.1.6. Morphology of the new phases. The new phases formed by the various consolidants were observed using a scanning electron microscope (SEM) with a Field Emission Gun (FEG) (Tescan Mira3). SEM observation was performed on fracture surfaces, obtained from the specimens that had been subjected to compressive strength, after sputter coating with graphite (Quorum sputter coater Q150R ES).

2.3.2. Compatibility

2.3.2.1. Color change (ΔE^*). The color change was calculated by determining the CIE Lab color parameters (L^* = black-white, a^* = green–red, b^* = blue–yellow) of untreated and treated specimens, by taking measurements in 3 areas for each sample with a NH310 colorimeter. The color difference between the untreated and the treated conditions was then calculated according to the formula $\Delta E^* = (\Delta L^{*2} + \Delta a^{*2} + \Delta b^{*2})^{1/2}$.

2.3.2.2. Pore size distribution. The alterations in open porosity and pore size distribution after consolidation were assessed by mercury intrusion porosimetry (MIP) by a Pascal 140 and 240 instrument (Thermo Scientific). The samples were obtained from the specimens that had been subjected to compressive strength, as a negligible influence of the mechanical test on the pore system and presence of cracks is expected, given the brittle nature of the three substrates. The MIP samples were obtained by always including the first 5 mm from the treated surface, as the greatest variations in pore size distribution were expected in this volume.

2.3.2.3. Water sorptivity and water absorption after saturation. The rate of water absorption (sorptivity) and the final amount of water absorbed after saturation were determined according to the European Standard EN 15801 [22], by letting water enter the specimens by capillarity through the treated surface.

2.3.2.4. Contact angle. The wettability of untreated and treated surfaces was assessed by measuring the contact angle (θ) formed by a drop of deionized water (1 μL volume), deposited on the sample surface using a syringe with a 0.72 mm wide needle. A photograph of the drop was

taken 5 s after its deposition and then analyzed by using the ImageJ software v1.46r to calculate the contact angle. The measurement was performed on marble and limestone specimens, while in the case of the mortar samples the higher surface roughness made the contact angle measurement impossible.

2.3.3. Durability

2.3.3.1. Freezing–thawing cycles. The permanence of the consolidating effect after accelerated ageing was assessed by subjecting the specimens to freezing–thawing cycles, performed by partly modifying the European Standard EN 12371 [23]. The specimens were initially saturated with deionized water for 3 days, then subjected to cycles of freezing at $-20 \pm 2^\circ\text{C}$ for 2 h and thawing in deionized water at $+20 \pm 2^\circ\text{C}$ for 2 h. In total, 130 cycles were performed for marble and limestone and 28 cycles for mortar, drying the specimens and measuring the progressive weight loss every 10 cycles for the stones and every cycle for the mortars. At the end of the cycles, the residual dynamic elastic modulus was evaluated as described above.

2.3.4. Sustainability

2.3.4.1. Global warming indicator (GW). The emission of greenhouse gases along the life cycle of the consolidants, expressed in terms of kg CO_2 equivalent, was considered as a representative parameter of the environmental dimension of sustainability. The quantification of the indicator for each consolidant was performed via life cycle assessment (LCA) according to ISO 14040:2006 [24]. The consolidation of 1 m^2 of substrate (marble, limestone or lime mortar) was assumed as the functional unit of the LCA. The required amount of each consolidant to fulfil the functional unit was directly derived from the product consumption determined experimentally on the three substrates for increasing number of brush strokes (see results in Section 3.1.1). Adopting a cradle-to-gate approach, the emissions of greenhouse gases occurring along the life cycle of each consolidant were estimated considering the following life cycle stages: (i) the production phase; (ii) the transportation phase; (iii) the use phase. The production phase involves the manufacturing of the consolidant and its solvent, according to the formulations introduced in Section 2.2, including the production of any precursor and energy input required for the consolidant manufacturing. The transportation phase includes both the delivery of the materials needed for the consolidant manufacturing and the delivery of the consolidant itself to the conservation site. The production of the required packaging (plastic buckets) is also accounted for in this phase. The use phase consists in the application of the consolidant onto the substrate, assumed to be performed following the same methods described in Section 2.2. The production of the auxiliary materials (e.g., cellulose pulp, limewater, Japanese paper, rinsing products) is accounted for in this phase. In addition, in the use phase, the release of volatile compounds from the application of the product on the substrate was also taken into account: for DAP, the release of carbon dioxide and ammonia resulting from the formation of calcium phosphates was considered [11].

As an example, Fig. 2 reports the product system considered for the life cycle of the DAP treatment, with an indication of the life cycle stages included in the analysis. The reported amounts of material and energy flows are related to the application to the limestone substrate with the highest number of brush strokes (i.e. until apparent refusal). Inventories for all the combinations of consolidants and substrates are listed in the Supplementary Material (Tables S1–S4), alongside relevant assumptions. Additional details on the life cycle inventory modelling of the synthesis of stone consolidants can be retrieved elsewhere [25]. Inventory data for common background unit processes (production of precursors and solvents, energy supply, transportation) were retrieved from life cycle inventory databases, viz. nodes of the European Platform on LCA [26], as reported in detail in the Supplementary Material.

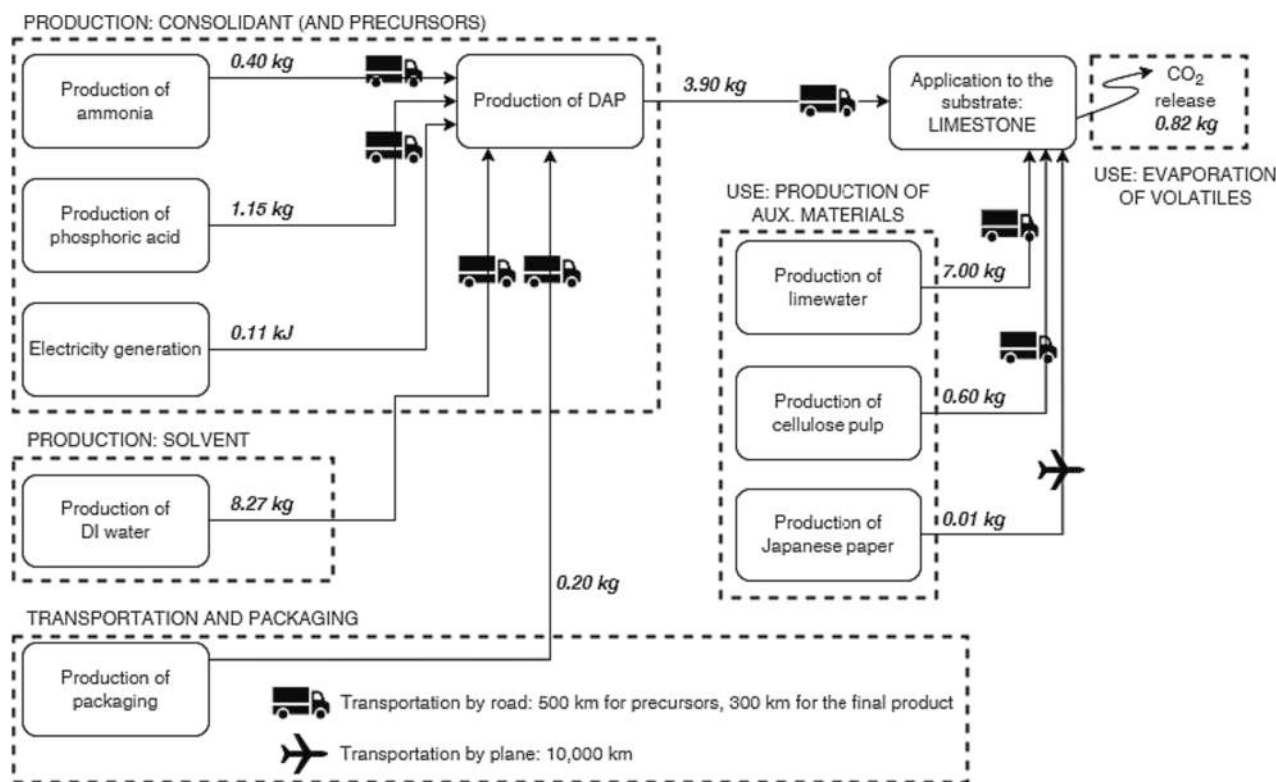


Fig. 2. Product system for the DAP treatment with quantified reference flows for the application to 1 m² of substrate surface. Case: application to limestone, until apparent refusal. Inventories for all the combinations of consolidants and substrates are reported in the Supplementary Material.

Following best practices in life cycle impact assessment methods [27], values of global warming potential over 100 years (GWP100) proposed by the Intergovernmental Panel on Climate Change [28] were assumed as characterization factors for the greenhouse gases in the computation of the GW indicator.

3. Results and discussion

3.1. Effectiveness

3.1.1. Product consumption and uptake

For each consolidant, the product consumption on the three substrates, as a function of the number of brush strokes, is reported in Fig. 3. For a given type of substrate and a given number of applications, the four consolidants exhibited comparable consumption, with some minor differences among the consolidants that reflect the different volatility of the respective solvents (the tendency to evaporate decreasing in the order acetone > ethanol > water > white spirit).

As a general trend, the product consumption progressively increased passing from marble to limestone to mortar. The low consumption on marble (which only required 7 brush strokes to reach apparent refusal) is consistent with the low open porosity of this stone (~3%). For the other two substrates, treated by 30 brush strokes to reach apparent refusal, the higher consumption was registered on mortar, which has a slightly lower open porosity (~21%) than limestone (~26%). This trend can be explained considering the respective pore size distributions: as detailed in Section 3.2.3, mortar has a bimodal distribution, with the bigger average pore size around 10 μm, while limestone has a unimodal distribution, with average pore size around 2 μm. Because liquids are absorbed more quickly into bigger pores [13], product absorption into the mortar specimens was easier and a higher consumption was registered.

Even though the product consumption on a given substrate was similar for the four consolidants, the product uptake by the specimens

was actually quite different, depending on the specific product (Fig. 3). The final product uptake is the result of a combination of competing factors, namely the viscosity of liquid consolidant, the concentration of the active principle and the volatility of the solvent present in each product. The DAP treatment (involving a DAP concentration of 396 g/L and water as solvent, leading a viscosity that is slightly higher than that of water) generally led to higher levels of product uptake, followed by ethyl silicate (containing 75 wt% of active principle and white spirit as solvent, leading to a viscosity that is 10 times higher than water). It is noteworthy that the relatively high viscosity of ES did not prevent it from achieving high values of products uptakes, thanks to a positive combination of the three factors. Nanolimes (5 g/L suspension in ethanol) and especially Paraloid B72 (5 wt% solution in acetone), both having viscosity similar to water, gave lower product uptakes, because only minimum amounts of active principle remained in the specimens after the solvent evaporation.

3.1.2. New phase morphology and composition

After curing and hardening, the consolidants caused the formation of new consolidating phases, with the morphology shown in Fig. 4 and the composition reported in Fig. 5.

The DAP treatment led to formation of calcium phosphates that appeared as new phases over the surface of calcite grains and inside intergranular fissures (Fig. 4). While these new calcium phosphates are generally reported to exhibit a flower-like morphology [10], in the present case they appeared as clusters on all the three types of substrate (in the case of marble, they were more easily distinguishable from the substrate). The reason for the different morphology is thought to be the method of application of the DAP solution (in the present study, brushing until apparent refusal, while previous studies mostly adopted immersion [11] or poulticing [17]). As highlighted in previous studies, the application method has a profound influence on the morphology and on the amount of the new consolidating phases, as well as on their strengthening efficacy [17,29,30]. Consistently, in a previous work

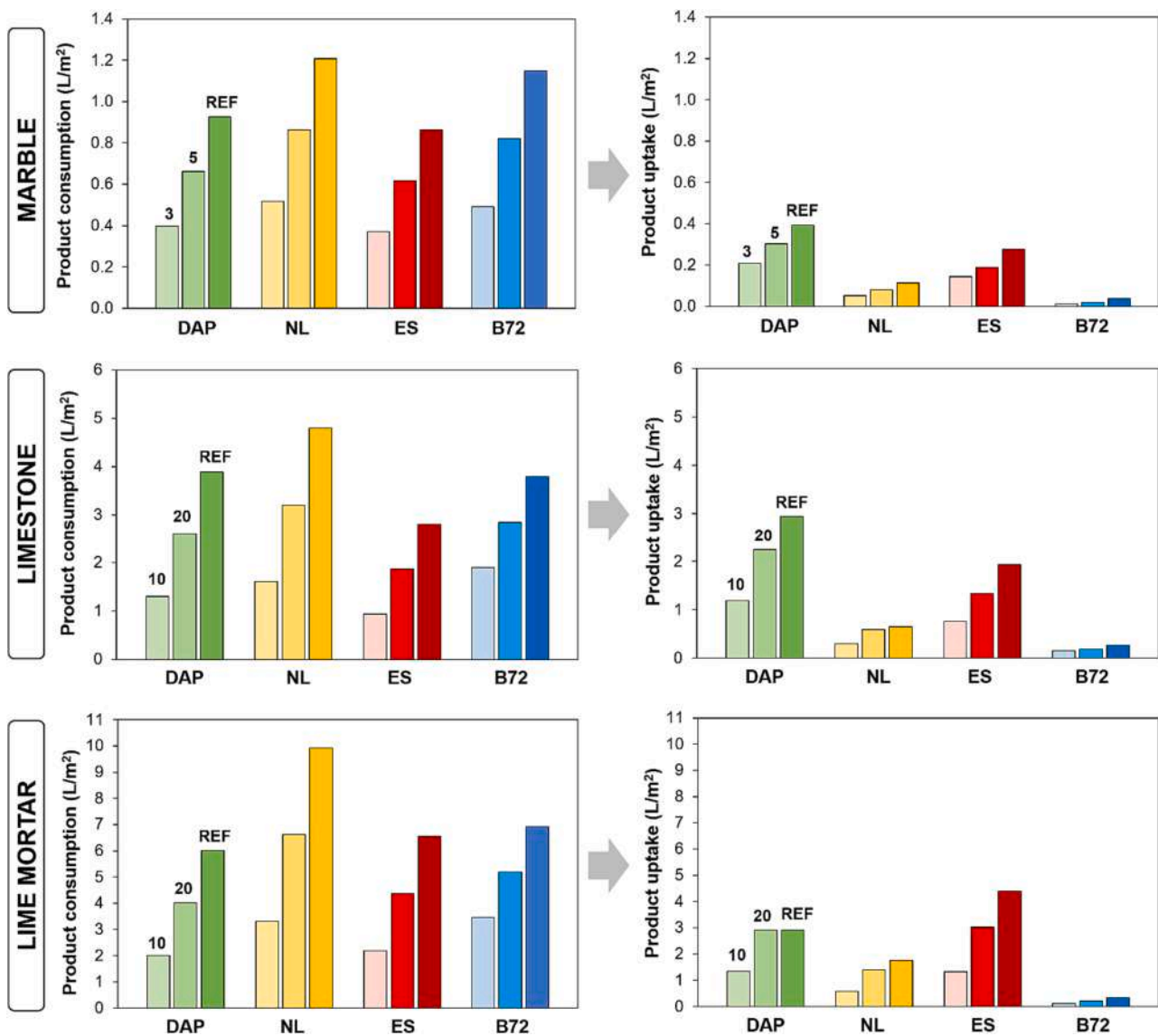


Fig. 3. Product consumption (left) and product uptake (right) for the three substrates.

where different application methods were compared, DAP application by poulticing was found to produce more abundant calcium phosphates than brushing, with also a clear difference in morphology (flower-like in the case of poulticing, smaller clusters in the case of brushing) [29]. In the present study, the new clusters observed by SEM were confirmed as calcium phosphates by FT-IR analysis, which revealed new bands attributable to calcium phosphates [30] at about 1028, 602 and 562 cm^{-1} in the spectra of all the three substrates, although limestone already contained some phosphate fractions that overlapped with those owing to the consolidant (Fig. 5). Because several different calcium phosphates, having similar FT-IR spectra [31], may be formed from the hardening reaction of DAP [10], conclusive identification was attempted by XRD. However, because of the small amount of new phases formed after the DAP treatment, their likely poor crystallinity and the threshold of detectability of XRD, no conclusive identification of the new calcium phosphates was possible (Fig. S1). Based on previous studies [10,32], formation of hydroxyapatite (HAP, $\text{Ca}_{10}(\text{PO}_4)_6(\text{OH})_2$), possibly coexisting with carbonate hydroxyapatite (C-HAP, $\text{Ca}_{10}(\text{PO}_4)_3(\text{CO}_3)_3(\text{OH})_2$) and/or octacalcium phosphate (OCP, $\text{Ca}_8\text{H}_2(\text{PO}_4)_6 \cdot 5\text{H}_2\text{O}$), is most likely. All these phases have lower water solubility than calcite, hence their formation can be considered as positive.

Nanolimes led to the formation of new calcium carbonate crystals,

which could be distinguished on the surface of marble (Fig. 4), while the more complex microstructure of limestone and mortar made their identification less straightforward. As expected, FT-IR did not reveal the presence of the new consolidating phases (Fig. 5), because their chemical composition is the same as that of the substrate. The complete conversion of the consolidant into calcium carbonate was also verified both by FT-IR (Fig. 5), where O-H stretching ($3600\text{--}3500\text{ cm}^{-1}$ [33]) owing to residual portlandite was not detected in any of the substrates, and by XRD (Fig. S1), where no residual portlandite was found as well.

Ethyl silicate led to formation of silica gel, clearly evidenced by new FT-IR bands at about 1080 and 460 cm^{-1} [34] in marble and mortar (Fig. 4), while limestone already contained quartzitic and apatitic fractions (main bands in the region of 1080 and 1030 cm^{-1} , respectively), which overlap with the new bands owing to the consolidant. In all cases, reactions between components of the substrate and the consolidant may also induce small modifications and displacement of IR peaks whose position depends on the chemical environment. Notably, no ethoxy groups owing to residual ethyl silicate were detected by FT-IR [35], even though the completion of the curing reactions of ethyl silicate are known to last much longer than the 4 weeks of curing adopted in this study [13]. This can be explained considering that the FT-IR samples were obtained from specimens that had been subjected to the water

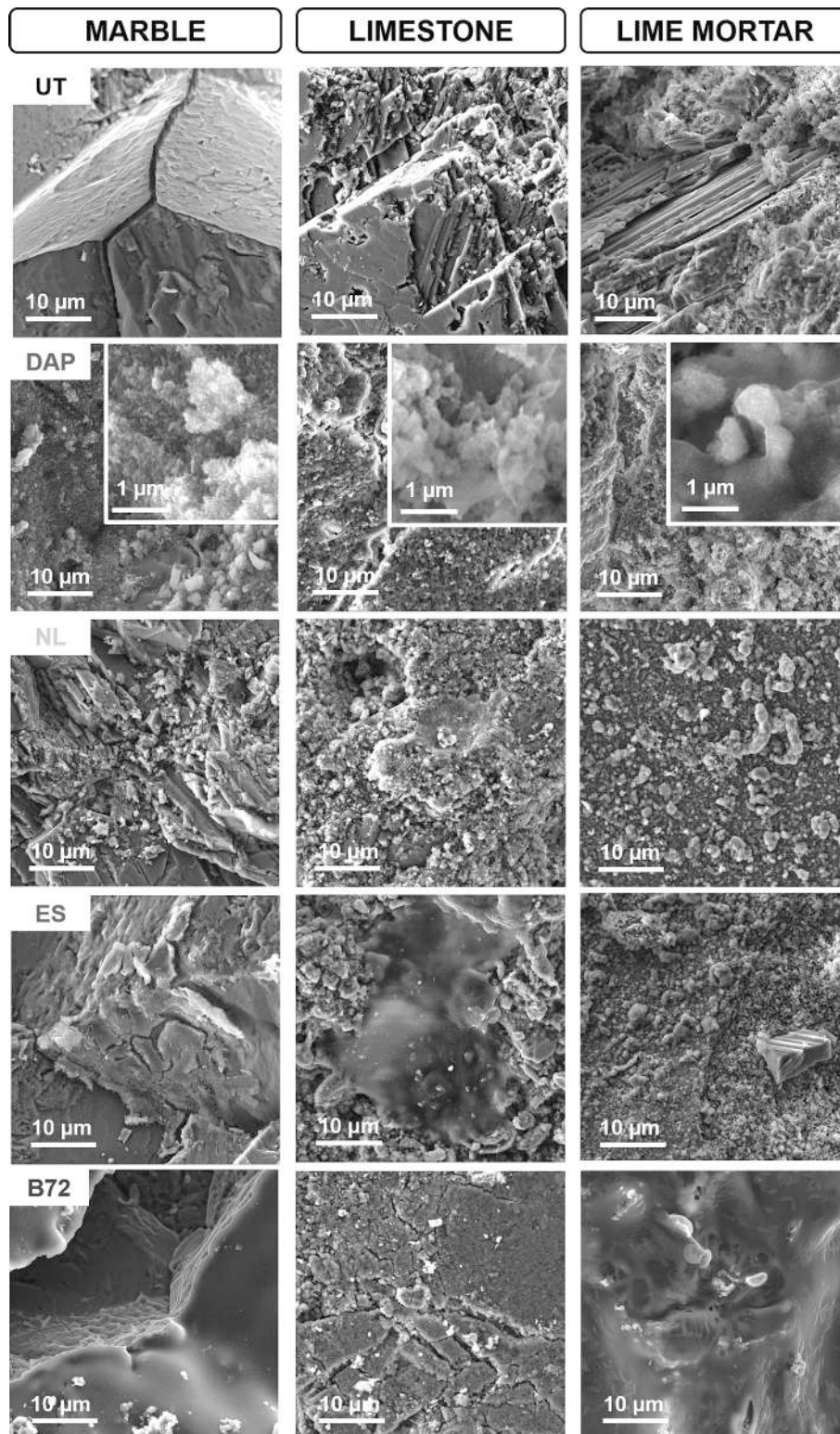


Fig. 4. SEM images of untreated and consolidated samples.

absorption test (cf. Section 2.3.1.5) and also considering that prolonged contact with water accelerates the curing reactions of ethyl silicate [35], so that only silica (i.e. the final product of ethyl silicate hydrolysis and condensation) was detected by FT-IR, with no residual ethoxy groups. It is also noteworthy that, in the case of the mortar sample, even though only bands owing to calcite were detected when the mortar was analyzed as a whole (Fig. 5), still traces of quartz were found by FT-IR

and by XRD in the aggregate used for the mortar preparation (in Fig. S1, quartz peaks are visible in some of the mortar samples, although not systematically). The presence of quarzitic fractions in the aggregate can explain the high consolidating ability registered in the prosecution of the study (Section 3.1.3). The newly formed silica gel can be clearly distinguished by SEM observation in the case of marble, where a tendency of the consolidant to detach from the calcite grains can be noticed

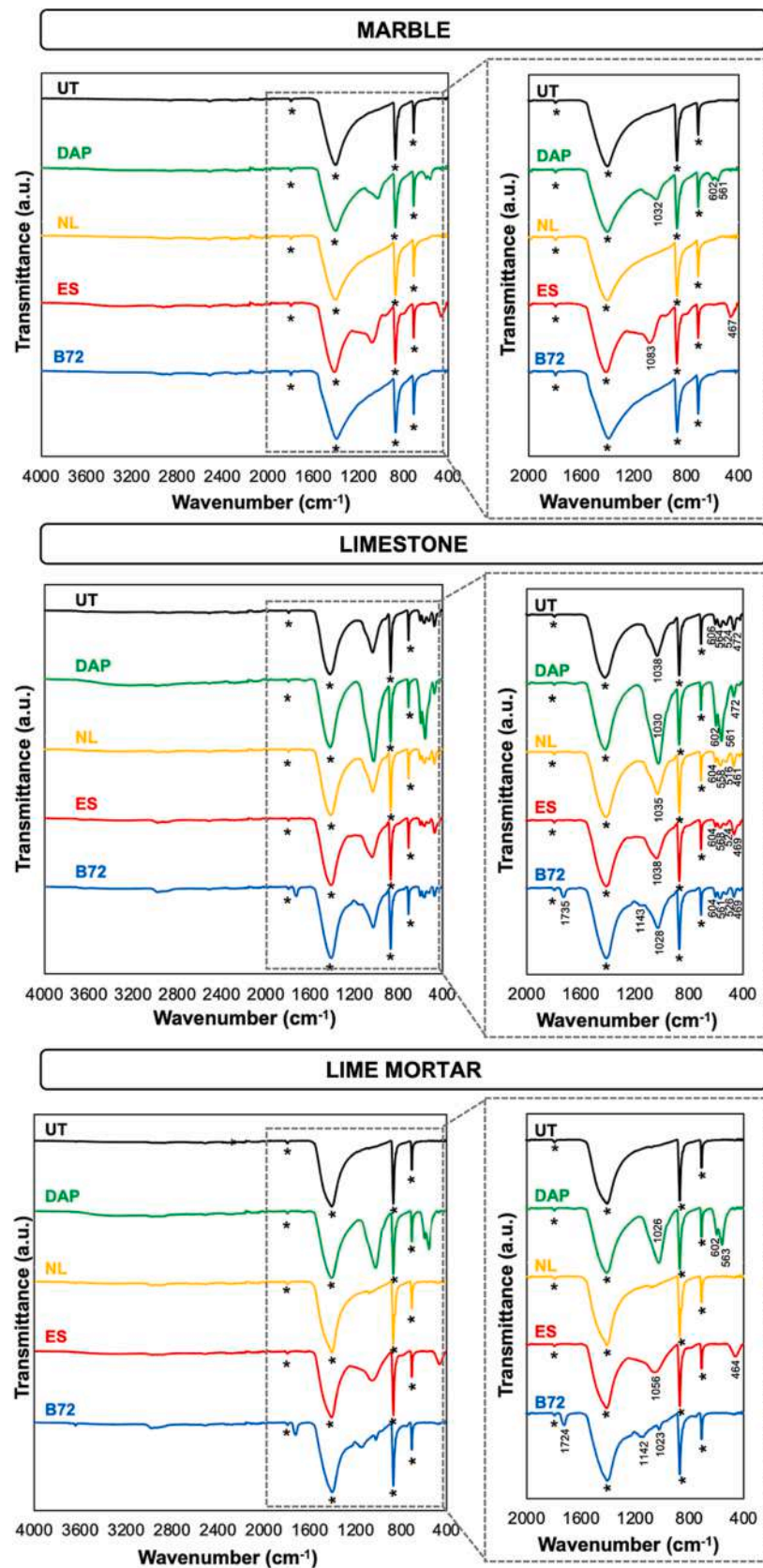


Fig. 5. FT-IR spectra of untreated and consolidated samples (bands owing to calcite are indicated by a star).

(Fig. 4).

The Paraloid B72 treatment induced new FT-IR bands at about 2960, 1730, 1140, 1025 cm^{-1} (Fig. 5) owing to acrylic resin [36,37]. The resin was clearly distinguishable by SEM observation, especially in the case of marble and mortar (Fig. 4).

3.1.3. Mechanical improvement

Thanks to their binding action after hardening, the four consolidants allowed for the mechanical improvement illustrated in Fig. 6, in terms of percentage increases in dynamic elastic modulus and compressive strength.

In the case of marble, the highest increase in E_d was produced by DAP, followed by ES, while NL and B72 had sensibly lower effect (Fig. 6). The very high levels of improvement in E_d (up to +3100% for DAP) can be explained considering the corresponding increases in ultrasonic pulse velocity (UPV), which is the most commonly used parameter to assess the deterioration of marble [38–40]. Indeed, a classification has been proposed by Köhler [41] to rank the state of conservation of marble from the condition of “disintegrated marble” ($UPV < 1.5 \text{ km/s}$) to that of “fresh marble” ($UPV > 5 \text{ km/s}$). In the present study, after consolidation the average UPV increased from 0.8

km/s (“disintegrated marble” condition) up to 4.8 km/s for DAP and 4.4 km/s for ES (in both cases, condition of “marble with increasing porosity”, for DAP very close to the condition of “fresh marble”). As E_d is calculated from UPV according to the formula $E_d = \rho \times UPV^2$ (where ρ is the geometric density), the high levels of improvement in E_d are explained.

Notwithstanding the comparable improvement in E_d caused by DAP and ES when applied by the highest number of brush strokes, the two consolidants led to different improvements in $\sigma_{c,DPT}$, in that DAP also caused a sensible $\sigma_{c,DPT}$ increase while the effectiveness of ES was significantly lower. This can be explained considering that ES is able to penetrate in depth in the intergranular fissures among calcite grains, thus immobilizing them and increasing the marble cohesion, but still the silica gel formed after hardening does not chemically bond to the calcitic substrate [13], as suggested in the present case by the detachment of the consolidant observed by SEM in the ES sample (Fig. 4).

In the case of limestone, DAP and ES were again the two consolidants that provided the highest improvements in both E_d and $\sigma_{c,DPT}$ (Fig. 6). Notably, while DAP was able to bring a substantial mechanical benefit even when applied by the lowest number of brush strokes (10), the effectiveness of ES highly depended on the amount of product applied:

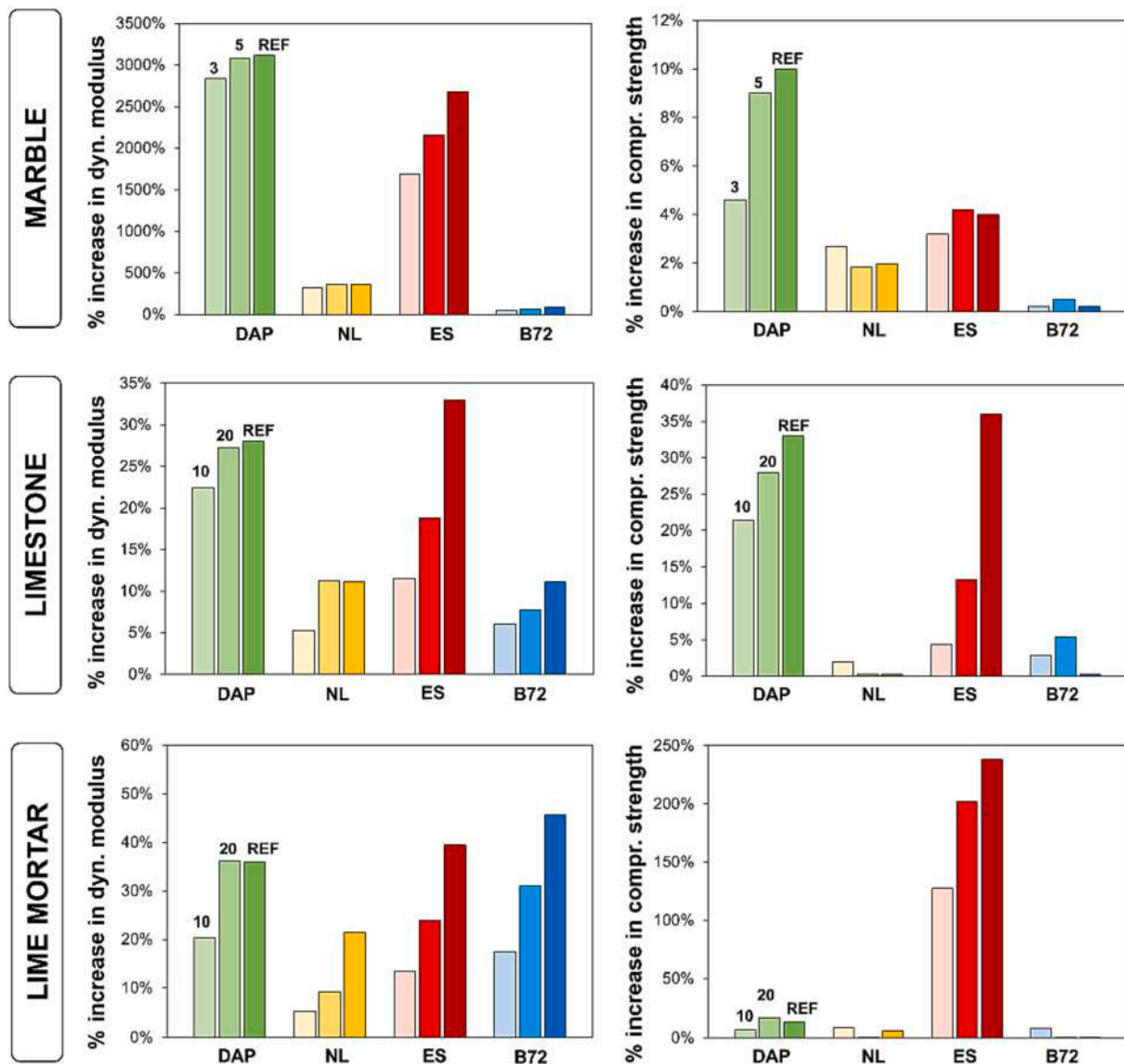


Fig. 6. Percentage increases in dynamic elastic modulus and compressive strength after consolidation, compared to the untreated condition.

basically no benefit was found when ES was applied by 10 brush strokes and only a modest improvement (not comparable to DAP) was registered for 20 brush strokes, while ES became competitive with DAP only for 30 brush strokes. The high effectiveness of ES on limestone can be ascribed to the presence of quartzitic fractions (Fig. 5), which can allow for some chemical bonding between the consolidant and the substrate [42–43].

In the case of lime mortar, the four consolidants caused substantially comparable increases in E_d , but the situation changed tremendously in terms of $\sigma_{c,DPT}$ (Fig. 6). ES brought by far the highest improvement in $\sigma_{c,DPT}$, the benefit increasing for increasing number of applications. Such a high consolidating effectiveness was unexpected in the case of the lime-based mortar specimens, but it can be explained considering that some quartzitic fractions (detected when the aggregate was analyzed alone by FT-IR) might allow for chemical bonding to the hardened consolidant [42–43]. Among the other treatments, DAP caused some noticeable increases in $\sigma_{c,DPT}$ (maximum +16 %), while lower improvements were registered for NL and B72 (Fig. 6).

3.2. Compatibility

3.2.1. Chemical compatibility of the new phases

Considering the mineralogical composition of the three substrates, primarily composed of calcium carbonate, the NL treatment can be considered as fully compatible in all the cases, because the final hardened consolidant has exactly the same composition as the substrate.

In the case of ES, the final hardened consolidant consists of amorphous silica, which has the same chemical composition as the quartzitic fractions that are naturally present in the limestone and in the aggregate used in the mortar, while in marble some quartzitic traces are present only as impurities (Fig. 5 and Fig. S1). Notwithstanding the similarity in chemical composition, the structure differs between the substrate (crystalline SiO_2) and the consolidant (amorphous SiO_2), which should be taken into consideration as the two phases may have different long-term behaviors.

By enlarging the concept of compatibility to the quality of not having negative consequences on the original substrate [44], the DAP treatment can also be considered as compatible with all the three substrates, as the final hardened consolidant (hydroxyapatite, possibly coexisting with carbonate hydroxyapatite and/or octacalcium phosphate) is a mineral that is naturally formed on the surface of carbonate substrates over time [45]. Natural patinas containing hydroxyapatite have been found to provide a protective action, so it is usually recommended that these patinas be not removed during restoration works [46].

The B72 treatment, leading to solidification of an ethyl-methacrylate copolymer once the solvent has evaporated, is the only treatment with scarce compatibility, as the final hardened polymer has been shown to suffer from poor resistance to photo-oxidative weathering, which results in irreversible transformations of the polymer and alteration of the consolidating properties [47,48].

3.2.2. Color change

The values of color change caused by the four consolidants, in comparison with the untreated references, are reported in Fig. 7, where the thresholds corresponding to the visibility by the human eye ($\Delta E^* = 2.3$ [49]) and the acceptability limit commonly adopted in the conservation field ($\Delta E^* = 5$ [50]) are also indicated.

In marble, DAP, NL and B72 induced color changes below the common acceptability limit, hence they can be considered as compatible from the aesthetic point of view. On the contrary, ES was responsible for a clearly visible color change (even for the lowest number of brush applications), mainly because of a decrease in the L^* parameter (i.e. darkening), which makes this consolidant scarcely compatible with marble. Darkening of ES-treated substrates has been extensively reported in the literature and attributed to the filling of pores with the hardened consolidant, which has a different refractive index compared to air that was filling the pores before consolidation [51]. The darkening

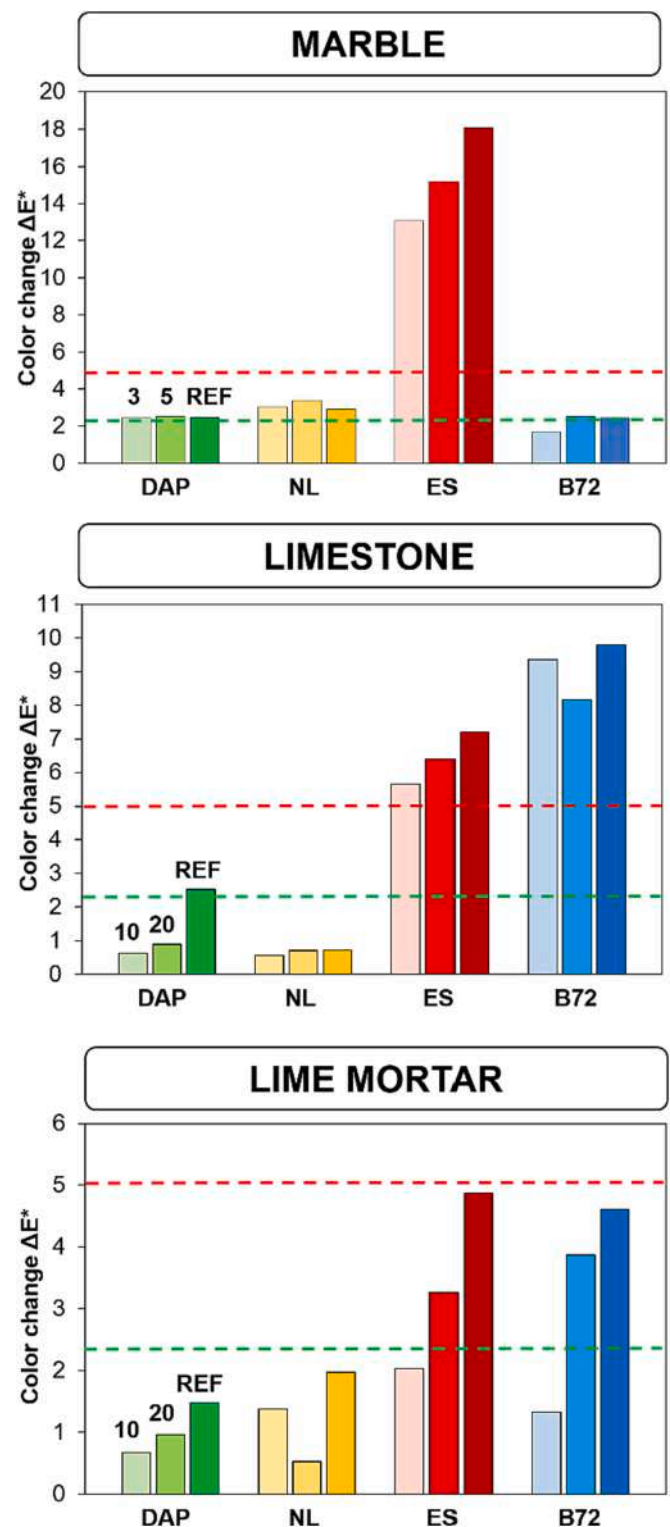


Fig. 7. Color changes after consolidation (the green dotted line indicates the visibility limit by the human eye, the red dotted line indicates the common acceptability limit). (For interpretation of the references to color in this figure legend, the reader is referred to the web version of this article.)

effect of ES, which is influenced by the initial color of the stone, the size of the pores and the texture of the substrate [51], was common to all the three substrates, as described in the following.

In the case of the limestone, ES and B72 caused color changes higher than the acceptability limit, for all the number of applications (Fig. 7).

ES was again responsible for visible darkening, although the darkening effect was lower on limestone (initially yellow) than on marble (initially white). B72 caused visible darkening and yellowing, which might have been favored by some accumulation of the resin on the treated surface (as also suggested by water absorption tests, discussed in Section 3.2.4), notwithstanding the removal of excessive product by acetone performed at the end of the brushing application (cf. Section 2.2). Differently, the DAP and NL treatments caused negligible color alterations, which were mostly below the detectability by the human eye.

The lime mortar was the only type of substrate where all the four consolidants caused acceptable color changes (Fig. 7), always below the common acceptability limit and always below the detectability limit by the human eye in the case of DAP and NL. The lack of significant color change after treatment, in spite of the initial white color like marble, might have been helped by the high porosity and coarse pore size of the mortar, which allow for easy in-depth penetration of the consolidants.

3.2.3. Pore size distribution

The effects of the consolidants on the pore size distribution of the three substrates are illustrated in Fig. 8, where one representative curve for each condition is reported in terms of cumulative pore volume and differential distribution of the intruded pore volume (measurements were performed on triplicate samples).

In marble, DAP and NL caused minor alterations, while B72 and especially ES caused pronounced reductions in open porosity, consistent with previous findings [52,53]. The significant pore occlusion caused by ES may be linked, on the one hand, to the high amount of active principle contained in the liquid consolidant and, on the other hand, to the small size of the SiO_2 particles formed after hardening. Actually, pore occlusion after consolidation is a key aspect in marble conservation, because experimental tests have shown that, when pores and cracks are completely filled with a stiff consolidant (e.g. silica gel), then the consolidated marble may be highly sensitive to thermal weathering, because calcite crystal deformation upon heating might be impeded [53]. As a result, marble treated with DAP (that does not significantly

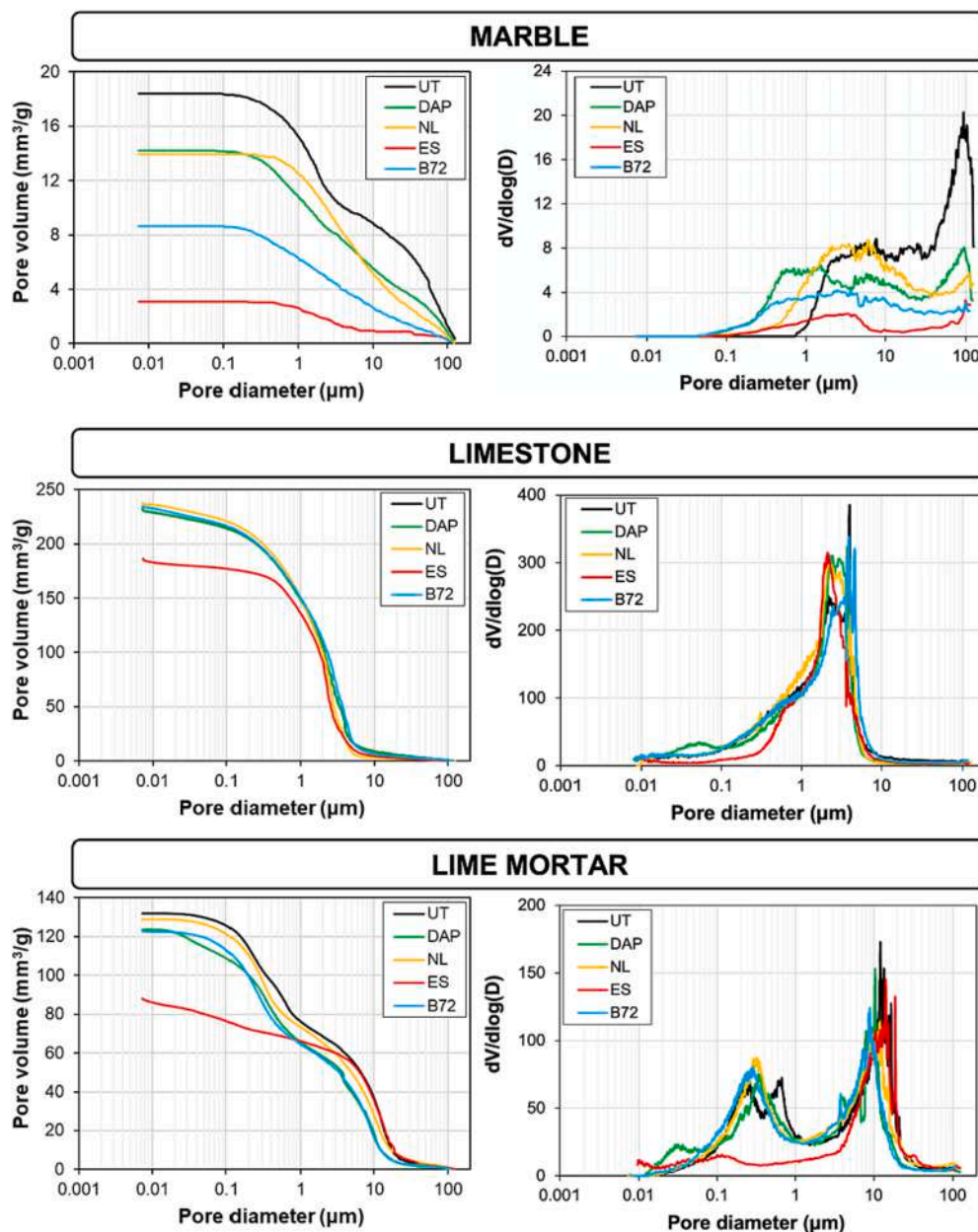


Fig. 8. Pore size distribution of the untreated and consolidated samples.

occlude pores) has been proved to resist heating–cooling cycles with limited damage [53], while ES-treated marble was severely affected by the same temperature cycles [53]. The damaging effect of temperature variations is lower when intergranular fissures are filled with a deformable consolidant, like Paraloid B72, because calcite crystal deformation is not impeded, although thermal damage may anyway be experienced, depending on the glass transition temperature of the organic resin [54].

In the case of limestone, initially exhibiting high open porosity, DAP, NL and B72 caused minor alterations to the pore size distribution, while

ES induced some noticeable pore occlusion, as also found in a previous study [3]. Similarly, in the case of lime mortar, ES was the only treatment causing a marked reduction in open porosity, with occlusion of pores below $\sim 4 \mu\text{m}$, while the other treatments led to limited changes. For both limestone and mortar, the alteration in the pore size distribution is a very important and delicate aspect, because the resistance of porous substrates to freezing–thawing cycles and salt crystallization cycles may actually be diminished after consolidation if a higher crystallization pressure is experienced. This may be the case because the crystallization pressure is higher in smaller pores [2], hence

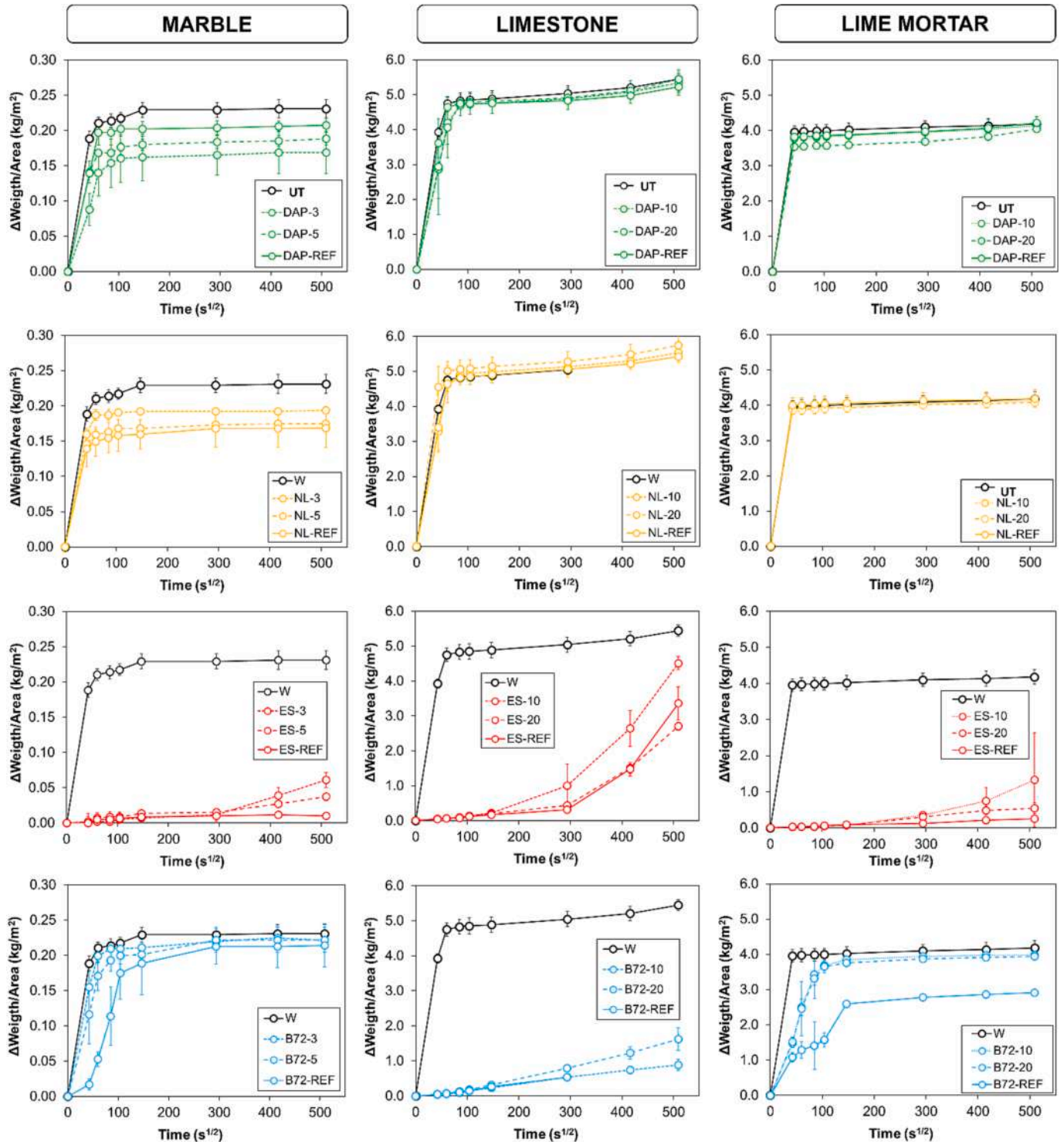


Fig. 9. Water sorptivity of the untreated and consolidated samples.

consolidants that modify the pore size distribution increasing the relative amount of smaller pores may be counterproductive.

To ascertain whether the alterations in pore size distribution registered after consolidation may negatively affect the durability of the substrate, specific tests were carried out (cf. Section 3.3).

3.2.4. Water transport properties

The curves illustrating the rate of water absorption as a function of time are reported in Fig. 9, while the total amount of water absorbed into the consolidated specimens is shown in Fig. 10, in comparison with the untreated references (UT). The contact angle of water with marble and limestone samples are reported in Fig. 11 (mortar samples had too high surface roughness).

In all substrates, the DAP and NL treatments caused minor alterations in sorptivity and water absorption, consistent with the limited alterations in pore size distribution (Fig. 8) and the lack of hydrophobic effects (Fig. 11), in agreement with previous studies [3,11,17].

On the contrary, at the beginning of the water absorption test the ES-treated specimens showed a marked hydrophobic behavior, with a little water absorption being registered only after prolonged contact with water (Fig. 9). This behavior, consistent with previous findings [3,35], is due to the residual presence of ethoxy groups on the treated surface, even after curing for 4 weeks [35]. Until ethoxy groups are completely replaced by hydroxyl groups, the treated surface remains hydrophobic. Prolonged contact with water allows to accelerate this process, so that at the end of the test the contact angle of ES-treated samples was similar to the untreated reference (Fig. 11). This can actually be exploited to speed up the hydrolysis-condensation reactions of ethyl silicate, for instance by applying a poultice of cellulose pulp and water [35] or water-ethanol solutions [55], so that the return to hydrophilic behavior and the full development of the consolidating capacity of ES can be achieved in a much shorter time [35].

Paraloid B72 slowed down the rate of water absorption and reduced the final amount of water penetrated into the substrates, as it caused hydrophobicity of the treated surface, as evidenced by the contact angle measurement (Fig. 11). The reduction in water absorption was most pronounced on limestone, compared to marble and mortar (Fig. 8), likely because, notwithstanding the removal of excess product from the treated surface by rinsing with acetone (cf. Section 2.2), some accumulation of acrylic resin occurred near the surface, which reduced water absorption (Fig. 9) and in turn increased the color change (Fig. 7).

It should be noted that the hydrophobic behavior induced by the consolidants (temporary in nature in the case of ES, long-lasting in the case of B72, Fig. 11) may actually be problematic, in case a source of water is present behind the consolidated layer (e.g. because rising damp is present). In such an event, water (possibly containing soluble salts) is prevented from exiting the stone, which may result in delamination of the hydrophobic layer, if the trapped water freezes or if salt crystallization occurs behind the consolidated layer [13]. The hydrophobicity of the substrate is thought to have contributed to the results of the durability test by freeze-thaw cycles, as described in the following paragraph.

3.3. Durability

To test the durability of the three substrates, when treated by the highest number of brush strokes (i.e. until apparent refusal), untreated and treated specimens were subjected to freezing-thawing cycles (130 for marble and limestone, 28 for mortar). The progressive weight loss as a function of the number of cycles is reported in Fig. 12, while the specimen appearance at the end of the cycles is shown in Fig. 13.

All marble specimens resisted well to freezing-thawing cycles for the first 60 cycles, when grain detachment started for untreated marble, which afterwards experienced progressive material loss. Specimens treated with NL and B72 started exhibiting material loss with only a slight delay compared to the untreated references, while only DAP and

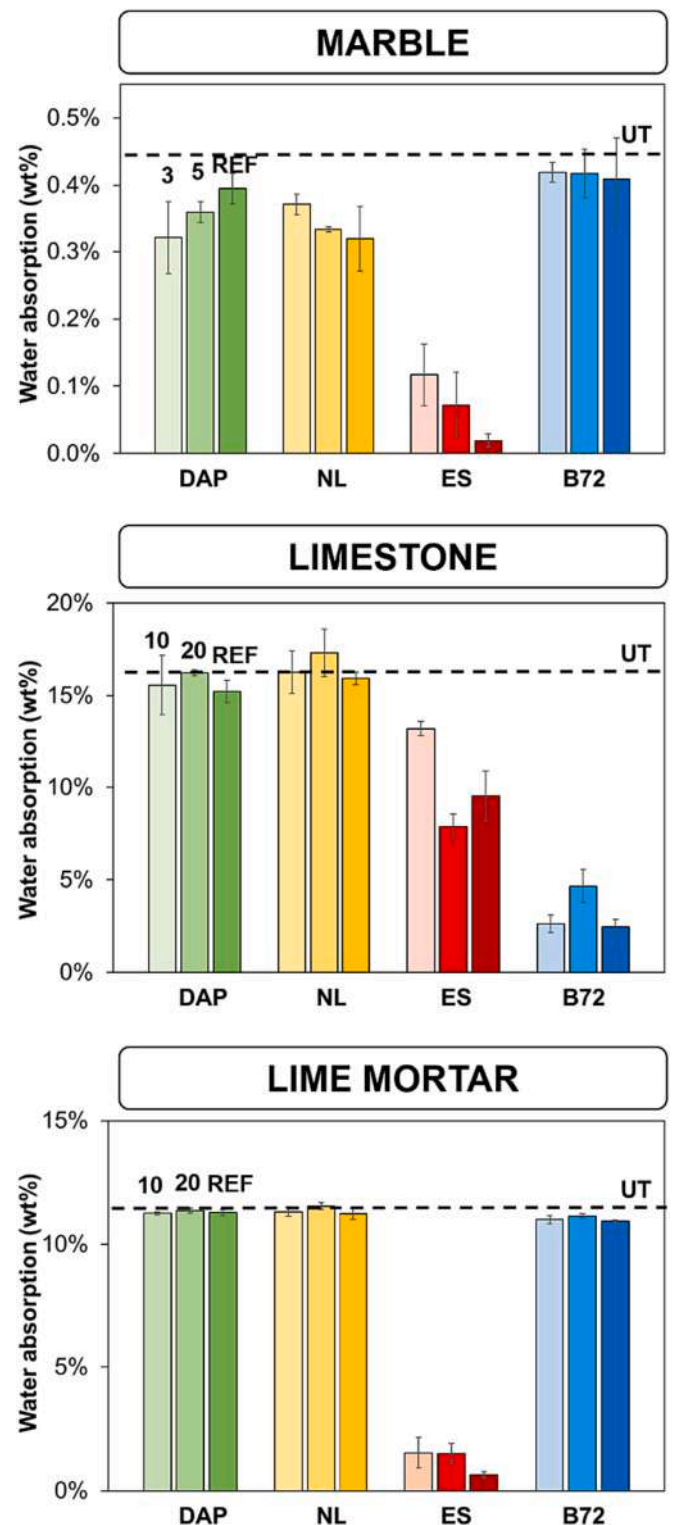


Fig. 10. Water absorption after saturation of the consolidated samples (the dotted lines represent the water absorption of the untreated references).

ES were able to significantly increase marble resistance to freeze-thaw, with negligible weight loss up to 130 cycles, as also confirmed by visual inspection at the end of the cycles (Fig. 13).

In the case of limestone, the untreated, B72- and ES-treated specimens started to lose weight already after the first 10 cycles, followed by the NL-treated ones that exhibited damage starting from the 20th cycle (Fig. 12). The low improvement in ice resistance provided by nanolimes

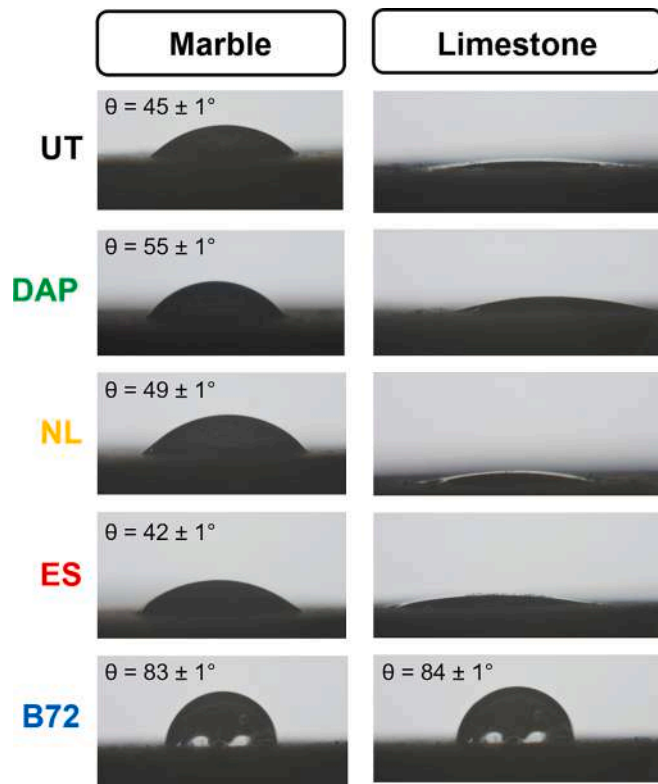


Fig. 11. Contact angle of untreated and consolidated samples (mortar samples had too high surface roughness to perform the contact angle measurements).

is in agreement with previous results on nanolime application to porous limestone, which actually suffered from increased salt crystallization pressure after consolidation [56]. Only the DAP specimens were able to stand all the 130 cycles without significant material loss, while extended detachments occurred in all the other specimens, as also evidenced by visual observation at the end of the cycles (Fig. 13). The high damage suffered by the specimens treated with ES, in spite of the initial strong improvement in mechanical properties right after consolidation (Fig. 6), is consistent with previous results reported in the literature on limestone consolidated by ethyl silicate and subjected to salt crystallization cycles [3,57]. Different factors may have contributed to the behavior registered in the present study, namely an increase in ice crystallization pressure after consolidation (similar to the increase in salt crystallization pressure due to the changes in pore size distribution caused by ethyl silicate [57]), and the temporary hydrophobic behavior caused by the ES-treatment. In fact, even though the hydrophilic behavior is re-established after prolonged contact with water [35], at the beginning of the freeze–thaw cycles the specimens still exhibited partly hydrophobic behavior (corresponding to the initial part of the test in Fig. 9): if water was able to penetrate into the sample through some discontinuity in the hydrophobic layer, then ice formation behind the consolidated layer likely occurred, with consequent stress and crack initiation. The same reasoning also applies to the case of B72, for which the hydrophobic behavior is long-lasting (Fig. 11).

In the case of lime mortar, the untreated specimens were the first to experience weight loss and fragment detachment, already after 8 cycles (Fig. 12). After a few cycles, the NL and then B72 specimens followed, while only the DAP and the ES ones were able to reach the end of the test (28 cycles) without significant material loss. Consistently, these specimens were the only ones maintaining the prismatic shape at the end of the cycles, while all the others suffered from huge material loss (Fig. 13).

The good durability of all the DAP-treated samples after immersion in water, followed by freeze–thaw cycles, is also a confirmation of the very low water solubility of the new calcium phosphates formed after

hardening (most likely, hydroxyapatite with the possible coexistence of carbonate hydroxyapatite and/or octacalcium phosphate, cf. Section 3.1.2).

3.4. Sustainability

As shown in Fig. 14, the environmental sustainability of the consolidants was assessed in terms of global warming (GW) indicator, calculated following a life cycle approach.

For each substrate, the GW related to each consolidant was quantified as a function of the number of brush strokes. DAP stands out as the consolidant associated to the lowest GW for all the substrates, followed by NL, whose GW score is on average 70% higher than DAP. ES and B72 have significantly higher impacts, ranging from 2 to 6 times those of DAP, depending on the substrate. The different scale of impacts across substrates is substantially proportional to the product consumption (Fig. 3).

To better analyze the differences between consolidants, Fig. 15 shows the breakdown of the GW impact into the life cycle stages introduced in Section 2.3.4 (production, transportation, and use). For the production stage, the impacts of the supply chains of the two macro-components of the product (the solvent and the consolidant itself) are shown separately. Transportation includes the production of packaging. For the use stage, the impacts related to the need of auxiliary materials and rinsing products (see description of the consolidating treatments in Section 2.2) are shown separately from the impacts associated to the direct release of greenhouse gases during application (only for DAP, carbon dioxide is released as a byproduct of the formation of calcium phosphates).

The repartition of the impacts across the life cycle stages shows significant differences between consolidants. For DAP, the highest share of the impact, ranging from 49 to 61% of the GW score, depending on the substrate, is related to the production of the consolidant itself, i.e., the synthesis of diammonium hydrogen phosphate, the related energy demand, and the production chain of the two precursors (ammonia and phosphoric acid). Only a negligible share of impact is related to the production of the solvent, which is water (<0.2%). The direct emission of CO₂ during application to the substrate accounts for 15–19% of the GW score, depending on the substrate. For NL, the reverse situation is observed: the synthesis of the nanolimes particles contributes for less than 4% to the total impact, while a share of the GW score ranging from 70 to 80%, depending on the substrate, is associated to the production of the solvent (ethanol). For ES, the production of the consolidant compound (ethyl silicate) is the main contributor to the GW indicator, but non-negligible shares of impact are associated with the production of the solvent (white spirit) and with the need for additional materials during application (additional white spirit for rinsing, mainly). For B72, the GW burden is mainly determined by the production of acetone, which is both the solvent in the consolidant formulation and the rinsing product used in the application stage. The production chain of the acrylic resin itself accounts for less than 10% of the impact in all the cases of application.

Based on the contribution analysis in Fig. 15, it is evident that the superior performance of DAP in terms of overall GW impact is given by (i) the use of water in place of an organic solvent, and (ii) the relatively low burden of diammonium hydrogen phosphate production.

It is also worth remarking that the environmental performance estimated by the LCA analysis has to be put into context and evaluated in combination with all the technical parameters of performance discussed above. In fact, based on the product consumption alone, a certain consolidant could appear as more sustainable and hence preferable, because it involves a lower GW, but in turn it could be basically ineffective in terms of mechanical strengthening. Here, the DAP treatment exhibited the highest mechanical effectiveness (Fig. 6) and the lowest GW burden (Fig. 14) of all the alternative consolidants for both the marble and limestone substrates, thus representing the preferred choice under both metrics. Conversely, for the lime mortar case, ES was shown to achieve a

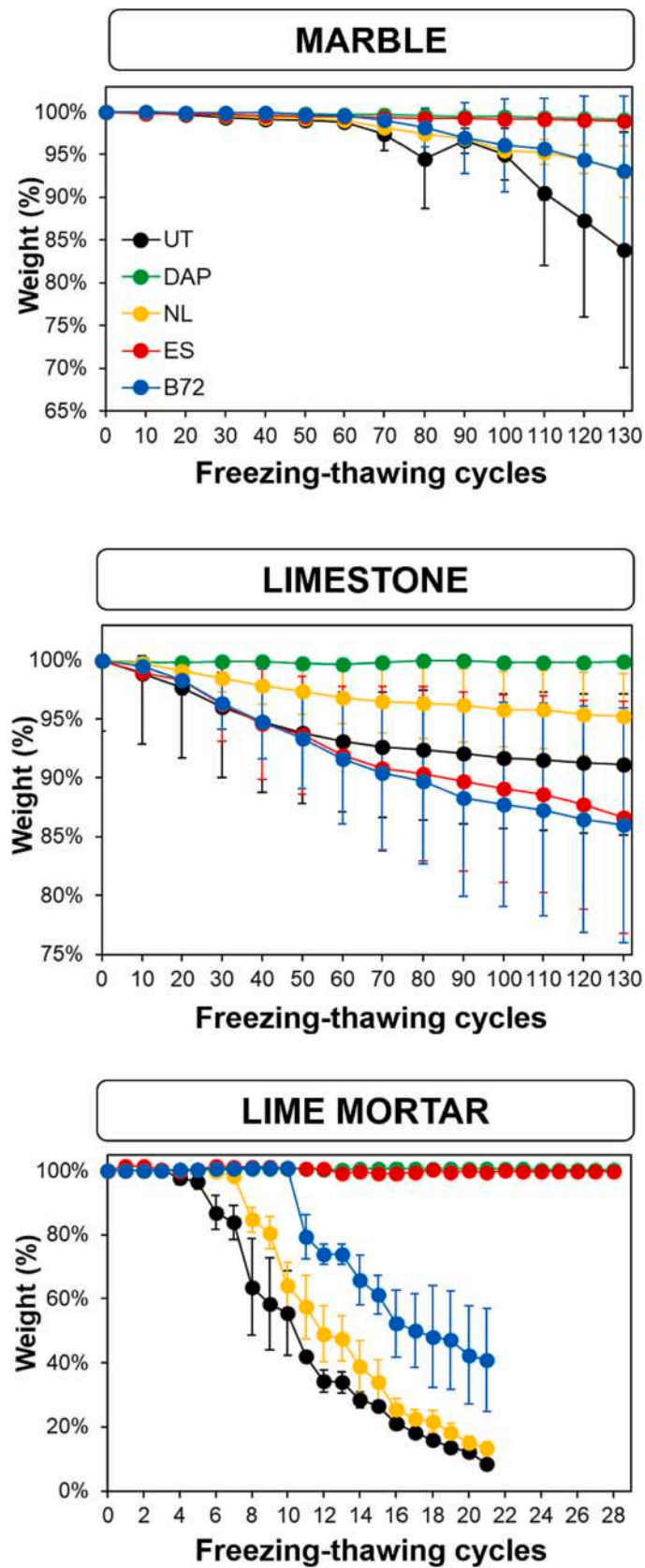


Fig. 12. Weight loss of untreated and consolidated samples during the freezing-thawing cycles.



Fig. 13. Appearance of untreated and consolidated samples at the end of the freezing-thawing cycles (130 cycles for marble and limestone, 28 cycles for lime mortars).

significantly higher consolidating performance than the other consolidants, but the associated GW impact is the highest. Having data on both the technical and environmental performance allows the practitioner to make an informed choice that might either prioritize one of the criteria or attempt a trade-off (e.g. selecting the most effective consolidant but using lower amounts).

Lastly, another aspect that should be considered is the interplay between environmental performance and durability of the various consolidants. In fact, depending on how quickly the consolidating effect is lost when the treated substrate is exposed to weathering processes, consolidants may need to be re-applied after different periods of time, thus determining a different GW over a given horizon of conservation. For instance, in the case of limestone, ES proved to be the most effective consolidant right after application (Fig. 6), but the weight loss of the ES sample was much quicker than that of DAP (Fig. 12), thus possibly requiring a more frequent re-application than DAP. Altogether, the good performance of DAP on the durability study (Section 3.3) suggests that the GW performance obtained in the studied application scenarios will be maintained even if multiple applications over time were to be considered.

4. Conclusions

The present study was aimed at providing a dataset that can guide the selection of the most suitable consolidant to be applied onto different carbonate substrates, namely marble, porous limestone and lime-based mortar. Four consolidants were considered: diammonium hydrogen phosphate (DAP), nanolimes (NL), ethyl silicate (ES) and acrylic resin (B72). Each consolidant was applied by brushing on each substrate in different amounts, to investigate the effects of reducing the product consumption with respect to the recommended application until apparent refusal. The consolidants were characterized in terms of

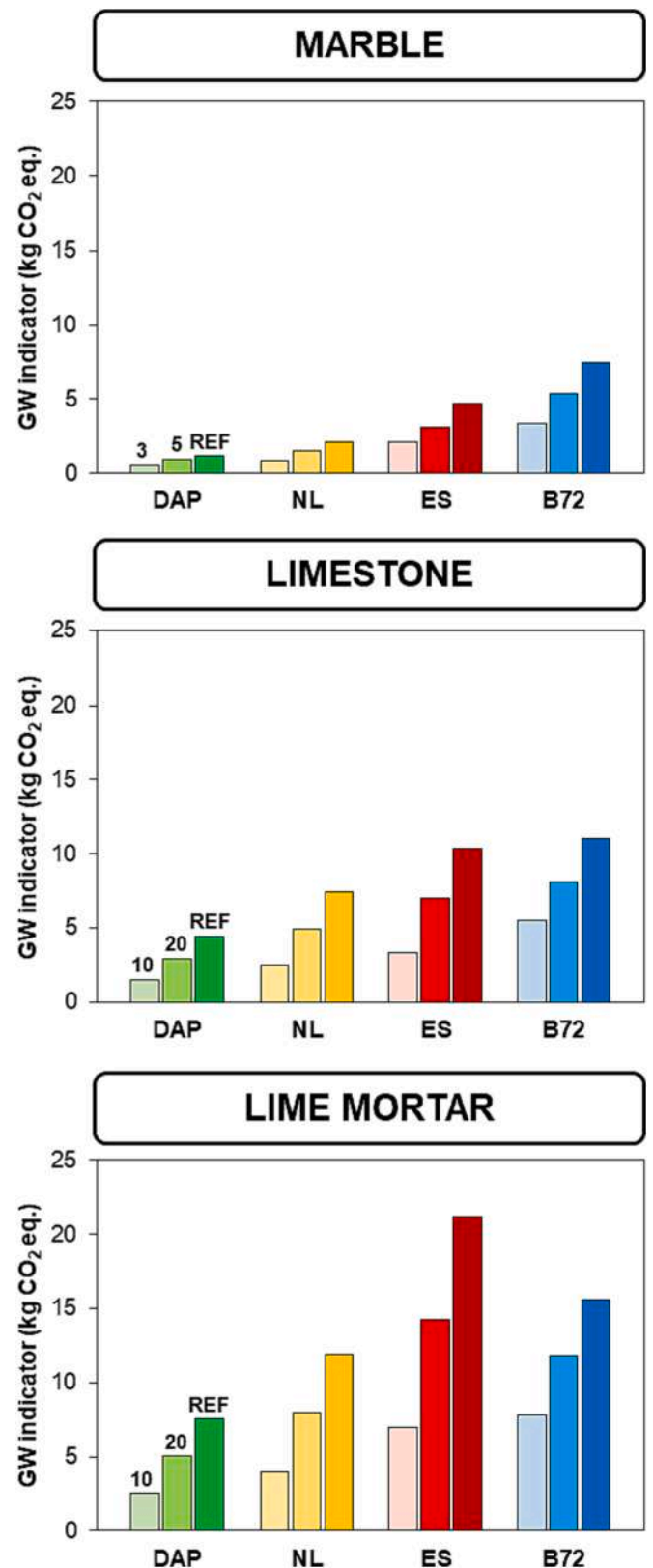


Fig. 14. Global warming (GW) indicator of the four consolidants onto the three substrates (treatment of 1 m² of surface).

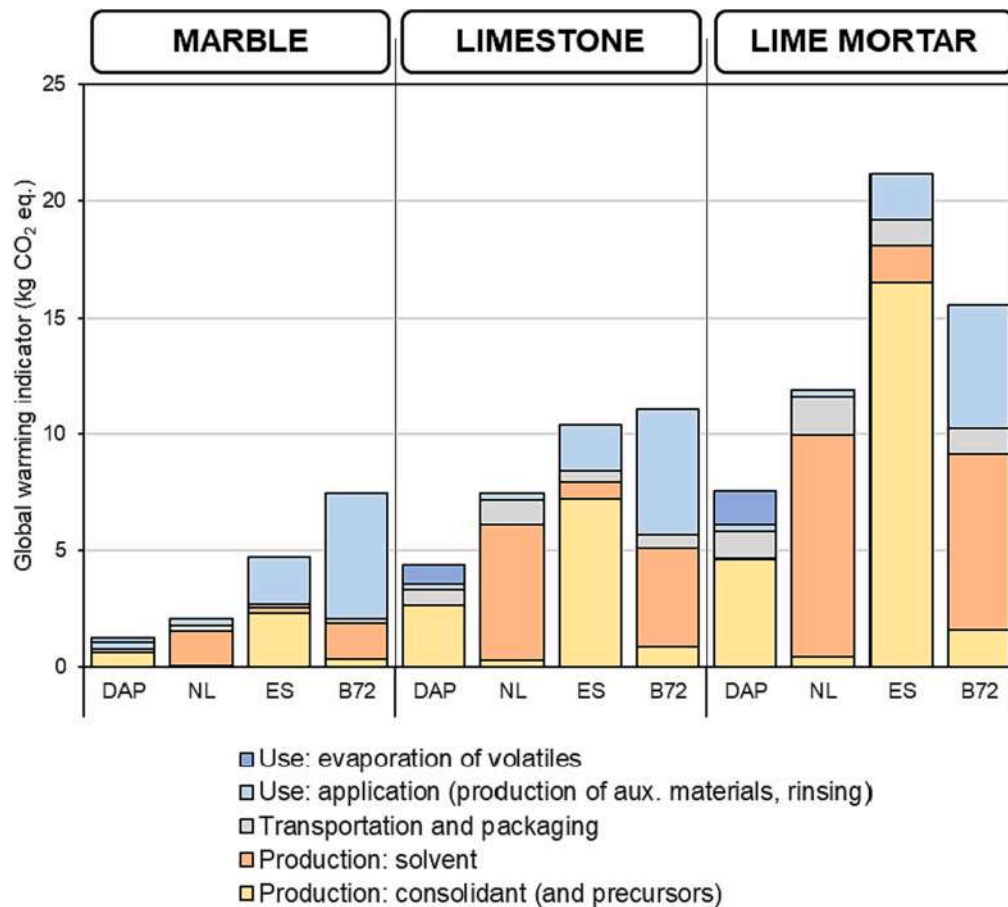


Fig. 15. Contribution analysis of the GW indicator (treatment of 1 m² of surface until apparent refusal).

mechanical effectiveness, compatibility with the substrate, durability to freezing-thawing cycles and sustainability, assessed by life cycle assessment (LCA). Based on the results obtained in this study, the following conclusions can be derived:

- The DAP treatment showed high mechanical effectiveness on all substrates, even when applied by a low number of brush strokes, thus resulting the most effective consolidant on marble and limestone and the second most effective on lime mortar, following ES. Compared to other treatments, DAP has the advantage of being effective after just a few days, instead of 4 weeks like ES and NL. DAP can be regarded as suitably compatible with these substrates, considering that the color change was always below the visibility limit by the human eye and alterations in pore size distribution and water transport properties were minor. The DAP treatment also showed remarkable durability, since all the DAP-treated substrates were able to reach the end of the accelerated durability test (130 freezing-thawing cycles for marble and limestone, 28 for mortar) basically without any weight loss. Finally, the DAP treatment can be accounted for the lowest global warming (GW) impact among the four investigated consolidants. Significantly, by coupling the LCA results with the findings on consolidation efficacy, DAP was able to provide the greatest mechanical improvement with the lowest GW. The good environmental suitability of DAP is largely to be ascribed to its aqueous solvent, the major contribution to its GW indicator coming from the production chain of diammonium hydrogen phosphate.
- Nanolimes showed very good compatibility on all the substrates, always causing color changes below the detectability by the human eye and minor alterations in water transport properties, but in turn they provided modest mechanical improvements, also when applied

in the highest amount. Some strengthening effect was registered only on lime mortar, while negligible effects were found on marble and limestone. Consistently, the NL treatment was unable to significantly extend the durability of any substrate when subjected to freezing-thawing cycles. In terms of sustainability, NL were responsible for GW indicators that were intermediate among the four consolidants (the greatest contribution to GW coming from ethanol used as solvent), but this has to be put into context with the lack of substantial mechanical effectiveness.

- ES proved to be very effective on limestone (containing quartz) and also on lime mortar (where the aggregate contained quarzitic fractions as well), while the strengthening effect was modest on marble. Notably, the effectiveness of ES significantly increased for increasing amount of product applied, so that on limestone ES became competitive with DAP only for high product consumption. ES caused visible color change, especially on marble that showed clear darkening, so it can be considered as aesthetically compatible only on lime mortar, where the color change was below the common acceptability limit. ES also caused significant pore occlusion and a marked hydrophobic behavior that started to disappear only after prolonged contact with water. The alterations in pore size distribution and water transport properties on limestone were presumably responsible for the poor durability after consolidation registered on this lithotype, while ES-treated marble and mortar were able to resist well freezing-thawing cycles. Because of the chemicals used for its production, ES proved to have a significantly higher GW impact than DAP or NL. As a consequence, ES appears competitive (limestone) or preferable (mortar) only when a high strengthening effect is needed, because DAP can generally provide high consolidation with lower GW than ES.

- The treatment based on acrylic resin caused unsatisfactory results in terms of effectiveness, because no substrate showed any substantial strengthening. While on marble and lime mortar modest color changes and alterations in water absorption were registered, B72-treated limestone showed visible chromatic alteration and reduction in water transport properties. The insufficient strengthening, combined with some hydrophobic behavior, was the cause of the negative performance in terms of durability of treated samples. Similarly to NL, B72 presents a GW footprint that is dominated by the contribution of the solvent, but the overall magnitude of its GW burden is higher and comparable to that of ES.

All things considered, the present study confirmed the potential of the DAP-based treatment, which shows several advantages over the alternative consolidants in terms of both technical performance and sustainability. In view of application to real cases, the DAP treatment can be considered as practical as the alternative commercial treatments: after application by brushing (as performed here), spraying or poulticing, it is recommended that the treated surface be wrapped in a plastic film for a few hours to avoid evaporation and then, after drying, covered with a poultice, which are all common operations in the conservation practice. The present findings also helped underline some of the strong points of ES (high strengthening efficacy also on carbonate substrates, when quartzitic fractions are present), but also important limitations (limited compatibility, possibly leading to scarce durability, as well as high global warming potential). Nanolimes and acrylic resin provided the least promising results.

Declaration of Competing Interest

The authors declare that they have no known competing financial interests or personal relationships that could have appeared to influence the work reported in this paper.

Data availability

Data will be made available on request.

Acknowledgements

Dr. Leonardo Borgioli (C.T.S. s.r.l., Italy) is gratefully acknowledged for kindly supplying the four consolidants. Prof. Matteo Minelli (University of Bologna) is gratefully acknowledged for precious suggestions for the determination of the consolidants viscosity. Dr. Riccardo Fabris (University of Bologna) is gratefully acknowledged for the determination of the surface roughness of the substrates. Dr. Giovanni Ridolfi (Centro Ceramico, Italy) is gratefully acknowledged for the contact angle measurements.

Appendix A. Supplementary data

Supplementary data to this article can be found online at <https://doi.org/10.1016/j.conbuildmat.2023.133599>.

References

- [1] S. Siegesmund, K. Ullemeyer, T. Weiss, E.K. Tschegg, Physical weathering of marbles caused by anisotropic thermal expansion, *Int. J. Earth Sci.* 89 (2000) 170–182, <https://doi.org/10.1007/s005310050324>.
- [2] G.W. Scherer, Crystallization in pores, *Cem. Concr. Res.* 29 (1999) 1347–1358, [https://doi.org/10.1016/S0008-8846\(99\)00002-2](https://doi.org/10.1016/S0008-8846(99)00002-2).
- [3] E. Sassoni, G. Graziani, E. Franzoni, An innovative phosphate-based consolidant for limestone. Part 1: effectiveness and compatibility in comparison with ethyl silicate, *Constr. Build. Mater.* 102 (2016) 918–930, <https://doi.org/10.1016/j.conbuildmat.2015.04.026>.
- [4] E. Sassoni, G. Graziani, E. Franzoni, An innovative phosphate-based consolidant for limestone. Part 2: Durability in comparison with ethyl silicate, *Constr. Build. Mater.* 102 (2016) 931–942, <https://doi.org/10.1016/j.conbuildmat.2015.10.202>.
- [5] F. Di Turo, L. Medeghini, How green possibilities can help in a future sustainable conservation of cultural heritage in Europe, *Sustainability* 13 (2021) 3609.
- [6] Y. Praticò, F. Caruso, R.J. Delgado, F. Girardet, E. Sassoni, G.W. Scherer, V. Vergès-Belmin, N.R. Weiss, G. Wheeler, R.J. Flatt, Stone consolidation: a critical discussion of theoretical insights and field practice, *RILEM Techn. Lett.* 4 (2019) 145–153, <https://doi.org/10.21809/rilemtechlett.2019.101>.
- [7] M. Favaro, P. Tomasin, F. Ossola, P.A. Vigato, A novel approach to consolidation of historical limestone: the calcium alkoxides, *Appl. Organometal. Chem.* 22 (2008) 698–704, <https://doi.org/10.1002/aoc.1462>.
- [8] P. Baglioni, E. Carretti, D. Chelazzi, Nanomaterials in art conservation, *Nat. Nanotechnol.* 10 (2015) 287–290, <https://doi.org/10.1038/nnano.2015.38>.
- [9] E. Franzoni, G. Graziani, E. Sassoni, G. Bacilieri, M. Griffa, P. Lura, Solvent-based ethyl silicate for stone consolidation: influence of the application technique on penetration depth, efficacy and pore occlusion, *Mater. Struct.* 48 (2015) 3503–3515, <https://doi.org/10.1617/s11527-014-0417-1>.
- [10] E. Sassoni, Hydroxyapatite and other calcium phosphates for the conservation of cultural heritage: a review, *Materials* 11 (2018) 557, <https://doi.org/10.3390/ma11040557>.
- [11] E. Sassoni, S. Naidu, G.W. Scherer, The use of hydroxyapatite as a new inorganic consolidant for damaged carbonate stones, *J. Cult. Herit.* 12 (2011) 346–355, <https://doi.org/10.1016/j.culher.2011.02.005>.
- [12] C. Rodriguez-Navarro, E. Ruiz-Agudo, Nanolimes: from synthesis to application, *Pure Appl. Chem.* 90 (2018) 523–550.
- [13] G.W. Scherer, G.S. Wheeler, Silicate consolidants for stone, *Key Eng. Mater.* 391 (2009) 1–25.
- [14] S.P. Koob, The use of paraloid B-72 as an adhesive: Its Application for Archaeological Ceramics and Other Materials, *Stud. Conserv.* 31 (1986) 7–14.
- [15] Calia A, Laurenzi Tabasso M, Maria Mecchi A, Quarta G (2014) The study of stone for conservation purposes: Lecce stone (southern Italy). *Geol Soc London, Spec Publ* 391:139 LP – 156. <https://doi.org/10.1144/SP391.8>.
- [16] A. Moropoulou, P. Maravelaki-Kalaitzaki, M. Borboudakis, A. Bakolas, P. Michailidis, M. Chronopoulos, Historic mortar technologies in Crete and guidelines for compatible restoration mortars, in: G. Biscontin, A. Moropoulou, M. Erdik, R.J. Delgado (Eds.), *Compatible Materials for the Protection of European Cultural Heritage PACT-55*, 1998, pp. 55–72.
- [17] A. Moropoulou, A.S. Cakmak, G. Biscontin, A. Bakolas, E. Zendri, Advanced Byzantine cement based composites resisting earthquake stresses: the crushed bricklime mortars of Justinian's Hagia Sophia, *Constr. Build. Mater.* 16 (2002) 543–552, [https://doi.org/10.1016/S0950-0618\(02\)00005-3](https://doi.org/10.1016/S0950-0618(02)00005-3).
- [18] Various Authors, “Corso sulla manutenzione di dipinti murali - Mosaici - Stucchi, Tecniche di esecuzione e materiali costitutivi”, Istituto Centrale per il Restauro, 1986.
- [19] E. Franzoni, E. Sassoni, G. Graziani, Brushing, poultice or immersion? The role of the application technique on the performance of a novel hydroxyapatite-based consolidating treatment for limestone, *J. Cult. Herit.* 16 (2) (2015) 173–184, <https://doi.org/10.1016/j.culher.2014.05.009>.
- [20] A.P. Ferreira Pinto, R.J. Delgado, Stone consolidation: The role of treatment procedures, *J. Cult. Herit.* 9 (2008) 38–53.
- [21] E. Sassoni, E. Franzoni, C. Mazzotti, Influence of sample thickness and capping on characterization of bedding mortars from historic masonries by double punch test (DPT), *Key Eng. Mater.* 624 (2015) 322–329, <https://doi.org/10.4028/www.scientific.net/KEM.624.330>.
- [22] European Standard EN 15801. Conservation of cultural property - Test methods - Determination of water absorption by capillarity (2009).
- [23] European Standard EN 12371. Natural stone test methods - Determination of frost resistance (2010).
- [24] International Standard Organization (ISO) 14040:2006 - Environmental management — Life cycle assessment — Principles and framework, International Organisation for Standardisation, Geneva (2006).
- [25] Dal Pozzo, A., Masi, G., Tugnoli, A., Sassoni, E., Towards Green Materials for Cultural Heritage Conservation: Sustainability Evaluation of Products for Stone Consolidation. In: Escalante-Garcia, J.I., Castro Borges, P., Duran-Herrera, A. (Eds) *Proceedings of the 75th RILEM Annual Week 2021*. RW 2021. RILEM Bookseries, vol 40, p. 751-760, 2023. Springer. DOI: 10.1007/978-3-031-21735-7_80.
- [26] European Platform on LCA (EPLCA), Life Cycle Data Network. Available at: <https://eplca.jrc.ec.europa.eu/LCDN/index.xhtml> (Last accessed: 23/03/2023).
- [27] M.Z. Hauschild, M. Goedkoop, J. Guinée, R. Heijungs, M. Huijbregts, O. Jolliet, M. Margni, A. De Schryver, S. Humbert, A. Laurent, S. Sala, R. Pant, Identifying best existing practice for characterization modeling in life cycle impact assessment, *Int. J. Life Cycle Assess.* 18 (2013) 683–697.
- [28] P. Forster, V. Ramaswamy, P. Artaxo, T. Bernsten, R. Betts, D.W. Fahey, J. Haywood, J. Lean, D.C. Lowe, G. Myhre, J. Nganga, R. Prinn, G. Raga, M. Schulz, R. Van Dorland, Changes in atmospheric constituents and in radiative forcing. Chapter 2, in: S. Solomon, D. Qin, M. Manning, Z. Chen, M. Marquis, K.B. Averyt, M. Tignor, H.L. Miller (Eds.), *Climate Change 2007: the Physical Science Basis. Contribution of Working Group I to the Fourth Assessment Report of the Intergovernmental Panel on Climate Change*, Cambridge University Press, Cambridge, 2007.
- [29] E. Sassoni, G. Ugolotti, M. Pagani, Nanolime, nanosilica or ammonium phosphate? Laboratory and field study on consolidation of a byzantine marble sarcophagus, *Constr. Build. Mater.* 262 (2020), 120784, <https://doi.org/10.1016/j.conbuildmat.2020.120784>.
- [30] A. Murru, R. Fort, Diammonium hydrogen phosphate (DAP) as a consolidant in carbonate stones: Impact of application methods on effectiveness, *J. Cult. Herit.* 42 (2020) 45–55, <https://doi.org/10.1016/j.culher.2019.09.003>.

- [31] I.A. Karampas, C.G. Kontoyannis, Characterization of calcium phosphates mixtures, *Vib. Spectrosc* 64 (2013) 126–133, <https://doi.org/10.1016/j.vibspec.2012.11.003>.
- [32] G. Ugolotti, G. Masi, E. Boanini, E. Sassoni, Influence of salt contamination on consolidation of slaked lime mortar by ammonium phosphate and nanolimes, *Constr. Build. Mater.* 35621 (2022), 129245, <https://doi.org/10.1016/j.conbuildmat.2022.129245>.
- [33] M. Khachani, A. El Hamidi, M. Halim, S. Arsalane, Non-isothermal kinetic and thermodynamic studies of the dehydroxylation process of synthetic calcium hydroxide Ca(OH)₂, *J. Mater. Environ. Sci.* 5 (2) (2014) 615–624.
- [34] F. Rubio, J. Rubio, J.L. Oteo, A FT-IR study of the hydrolysis of tetraethylorthosilicate (TEOS), *Spectrosc. Lett.* 31 (1) (1998) 199–219, <https://doi.org/10.1080/00387019808006772>.
- [35] E. Franzoni, G. Graziani, E. Sassoni, TEOS-based treatments for stone consolidation: acceleration of hydrolysis-condensation reactions by poulticing, *J. Sol-Gel Sci. Technol.* 74 (2015) 398–405, <https://doi.org/10.1007/s10971-014-3610-3>.
- [36] E. Carretti, D. Chelazzi, G. Rocchigiani, P. Baglioni, G. Poggi, L. Dei, Interactions between nanostructured calcium hydroxide and acrylate copolymers: implications in cultural heritage conservation, *Langmuir* 29 (2013) 9881–9890, <https://doi.org/10.1021/la401883g>.
- [37] O. Chiantore, M. Lazzari, Photo-oxidative stability of paraloid acrylic protective polymers, *Polymer* 42 (1) (2001) 17–27.
- [38] T. Weiss, P.N.J. Rasolofosaon, S. Siegesmund, Ultrasonic wave velocities as a diagnostic tool for the quality assessment of marble; in Natural stone, weathering phenomena, conservation strategies and case studies, *Geol. Soc. Lond. Spec. Publ.* 205 (2002) 149–164.
- [39] A. Luque, E. Ruiz-Agudo, G. Cultrone, E. Sebastián, S. Siegesmund, Direct observation of microcrack development in marble caused by thermal weathering, *Environ. Earth Sci.* 62 (2011) 1375–1386, <https://doi.org/10.1007/s12665-010-0624-1>.
- [40] J. Ruedrich, C. Knell, J. Enseleit, Y. Rieffel, S. Siegesmund, Stability assessment of marble statues of the Schlossbrücke (Berlin, Germany) based on rock strength measurements and ultrasonic wave velocities, *Environ. Earth Sci.* 69 (2013) 1451–1469, <https://doi.org/10.1007/s12665-013-2246-x>.
- [41] W. Köhler, Preservation problems of Carrara marble sculptures: Potsdam-Sanssouci (“radical structural destruction” of Carrara marble). 1988. VI International Congress on Deterioration and Conservation of Stone, *Proc Actes*, 653–662.
- [42] P. Maravelaki-Kalaitzaki, N. Kallithrakas-Kontos, Z. Agioutantis, S. Maurigiannakis, D. Korakaki, A comparative study of porous limestones treated with silicon-based strengthening agents, *Prog. Org. Coat.* 62 (2008) 49–60, <https://doi.org/10.1016/j.porgcoat.2007.09.020>.
- [43] S. Columbu, C. Lisci, F. Sitzia, G. Buccellato, Physical–mechanical consolidation and protection of Miocene limestone used on Mediterranean historical monuments: the case study of Pietra Cantone (southern Sardinia, Italy), *Environ. Earth Sci.* 76 (2017) 148, <https://doi.org/10.1007/s12665-017-6455-6>.
- [44] K. Van Balen, I. Papayanni, R. Van Hees, L. Binda, A. Waldum, Introduction to requirements for and functions and properties of repair mortars, *Mater. Struct.* 38 (2005) 781–785.
- [45] P. Maravelaki-Kalaitzaki, Black crusts and patinas on Pentelic marble from the Parthenon and Erecteum (Acropolis, Athens): characterization and origin, *Anal. Chim. Acta* 532 (2005) 187–198.
- [46] Giusti A. La competenza umanistica. In: Tiano P, Pardini C, editors. *Le patine – Genesi, significato, conservazione*, Proceedings of the Workshop “Le patine – Genesi, significato, conservazione”, 4–5 May 2004, Florence, Italy, Nardini Editore, Florence; 2005, p. 77–82.
- [47] M. Favaro, et al., Evaluation of polymers for conservation treatments of outdoor exposed stone monuments. Part I: Photo-Oxidative Weathering, *Polymer Degradat. Stability* 91 (2006) 3083–3096.
- [48] M. Favaro, et al., Evaluation of polymers for conservation treatments of outdoor exposed stone monuments. Part II: photo-oxidative and salt-induced weathering of acrylic-silicone mixtures, *Polymer Degrad. Stability* 92 (2007) 335–351.
- [49] G. Sharma, *Color fundamentals for digital imaging. Digital Color Imaging Handbook*, CRC Press, Boca Raton, FL, USA, 2003.
- [50] J.D. Rodrigues, A. Grossi, Indicators and ratings for the compatibility assessment of conservation actions, *J. Cult. Herit.* 8 (2007) 32–43, <https://doi.org/10.1016/j.culher.2006.04.007>.
- [51] G. Wheeler, Alkoxysilanes and the Consolidation of Stone, vol. 46, no. 2. 2005.
- [52] E. Sassoni, G. Graziani, E. Franzoni, Repair of sugaring marble by ammonium phosphate: Comparison with ethyl silicate and ammonium oxalate and pilot application to historic artifact, *Mater. Des.* 88 (2015) 1145–1157, <https://doi.org/10.1016/j.matdes.2015.09.101>.
- [53] Sassoni E., Andreotti S., Scherer G.W., Franzoni E., Siegesmund S., Bowing of marble slabs: can the phenomenon be arrested and prevented by inorganic treatments?, *Environ. Earth Sci.*, vol. 77, no. 10, 2018, doi: 10.1007/s12665-018-7547-7.
- [54] J. Menningen, E. Sassoni, R. Sobott, S. Siegesmund, Constraints of the durability of inorganic and organic consolidants for marble, *Environ. Earth Sci.* 80 (10) (2021) 1–19, <https://doi.org/10.1007/s12665-021-09664-w>.
- [55] Naidu S, Liu C, Scherer GW. New techniques in limestone consolidation: hydroxyapatite-based consolidant and the acceleration of hydrolysis of silicate-based consolidants. *J. Cult. Herit.* doi: 10.1016/j.culher.2014.01.001.
- [56] S.A. Ruffolo, et al., Efficacy of nanolime in restoration procedures of salt weathered limestone rock, *Appl. Phys. A Mater. Sci. Process.* 114 (3) (2014) 753–758, <https://doi.org/10.1007/s00339-013-7982-y>.
- [57] S.A. Ruffolo, et al., New insights on the consolidation of salt weathered limestone: the case study of Modica stone, *Bull. Eng. Geol. Environ.* 76 (1) (2017) 11–20, <https://doi.org/10.1007/s10064-015-0782-1>.